Analysis of Inching for Planetary Rover Exploration

Karen Orton

CMU-RI-TR-19-41

May 2019

School of Computer Science
Carnegie Mellon University
Pittsburgh, PA 15213

Thesis Committee:
David Wettergreen (Advisor)
Dimitrios (Dimi) Apostolopoulos
Eugene Fang

Submitted in partial fulfillment of the requirements for the degree of Master of Science.

Abstract

Inching, also called push-rolling, is method of moving for vehicles that can change the position of their wheels relative to their body. Like an inchworm, it is possible to hold some wheels stationary while advancing the others and the body. In this research a test apparatus capable to independently controlling wheel speed and body-relative position was designed, built, and used to measure and understand inching, particularly as it applies to traction, climbing, and sinkage for planetary rovers. Inching is shown to produce dramatically better performance than nominal mobility methods in loose soil at slip values above 20%. Tractive performance is shown to be related to wheel slip, even when inching. Therefore Inching can induce wheel slip, even when there is little vehicle slip, to increase tractive performance. Inching, as a method of mobility, shows great promise as a way to climb steeper hills safely with planetary rovers.

Acknowledgments

This work was supported in part by the Jet Propulsion Lab under grants 1516288 and 1612701 and SURP award 1540595.

I would like to thank the members of the thesis committee for their time and support of this research. Thank you David Wettergreen of Carnegie Mellon University (Advisor); Dimitrio (Dimi) Apostolopoulos of Carnegie Mellon University; Eugene Fang PhD Student at Carnegie Mellon University.

This thesis could not have been completed without the contributions of many individuals. David Kohanbash and Warren (Chuck) Whittaker of Carnegie Mellon University. Along with Scott Moreland of the Jet Propulsion Laboratory are to be recognized for their major contributions to the research presented in this document.

Contents

List of Figures

Chapter 1

Introduction

1.1 Mobility Systems for Planetary Rovers

A major area of research for planetary robotics is the design of their mobility system. It is important for planetary rovers to be able to drive through loose sand and to be able to climb up slopes, because both terrains are common on Mars. Any rover that wants to explore this planet must be able to traverse these two types of terrains.

Robots were first utilized for planetary exploration on November 17, 1970 when the Soviet Lunokhod 1 landed on the moon [10]. This is a unique use case for robotics as it is a task that cannot presently be completed by humans. Planetary rovers can provide invaluable scientific insights to the entire world that can be collected any other way. Planetary rovers typically land on a planetary body and then proceed to drive around collecting scientific data. Scientists and software designate locations that are of interest [11] and the robot will then drive hours if not days, weeks, or months to get to the location of interest to collect the desired data. These locations are commonly restricted by robotic engineers who determine which locations are safely reachable by the rover. Commonly there are scientifically interesting locations that are never visited because the rover can not safely reach them, limiting the scientific potential of missions[12]. Therefore the more easily and safely a robot can traverse steep slopes and deep sand, the more scientific areas a robot will be allowed to drive to.

The key to success for the two twin rovers that explored Mars, Spirit and Opportunity, was the design and operation of their mobility systems [13]. Their mobility systems were designed and tested for three main challenges, steep hills, loose soils, and large obstacles. Their mobility systems are a rocker-bogie design that allow the rovers to easily traverse over obstacles that are more than a wheel diameter in size. Figure 1.1 shows testing that was completed with a rover analogue driving through some deep soil.

Figure 1.1: Spirit and Opportunity rover analogue being tested driving through deep soil [1]

A large part of Mars is covered in this high sinkage, loose soil and therefore it is important for any rover driving on the planet to be able to traverse this type of soil. Unfortunately Spirit's mission ended when it became permanently entrapped in deep soil. An artists rendition of this situation is shown in Figure 1.2. This is a very costly issue, as it was the end of an expensive mission, therefore not getting entrapped in sand is an important attribute of any planetary rover mobility system.

Figure 1.2: Artist's rendition of the Spirit rover entrapped in sand [2]

When designing the mobility system for the rover Curiosity, testing was completed to understand how the vehicle would perform in various terrains and on many different slopes [13]. An example showing a mock up curiosity rover vehicle attempting to climb a hill for testing is shown in Figure 1.3.

Figure 1.3: Test vehicle at JPL attempting to climb a hill [3]

Figure 1.4 shows the consequences of not being able to climb a steep hill on Mars. This image shows tracks from Curiosity trying to climb a hill and then tracks coming back down the hill as it could not climb the whole thing. This would likely cause the rover to spend more time planning and driving around the hill it could not climb over. Again a costly problem when the goal of the mission is not spending time driving but to be spending time doing invaluable science experiments.

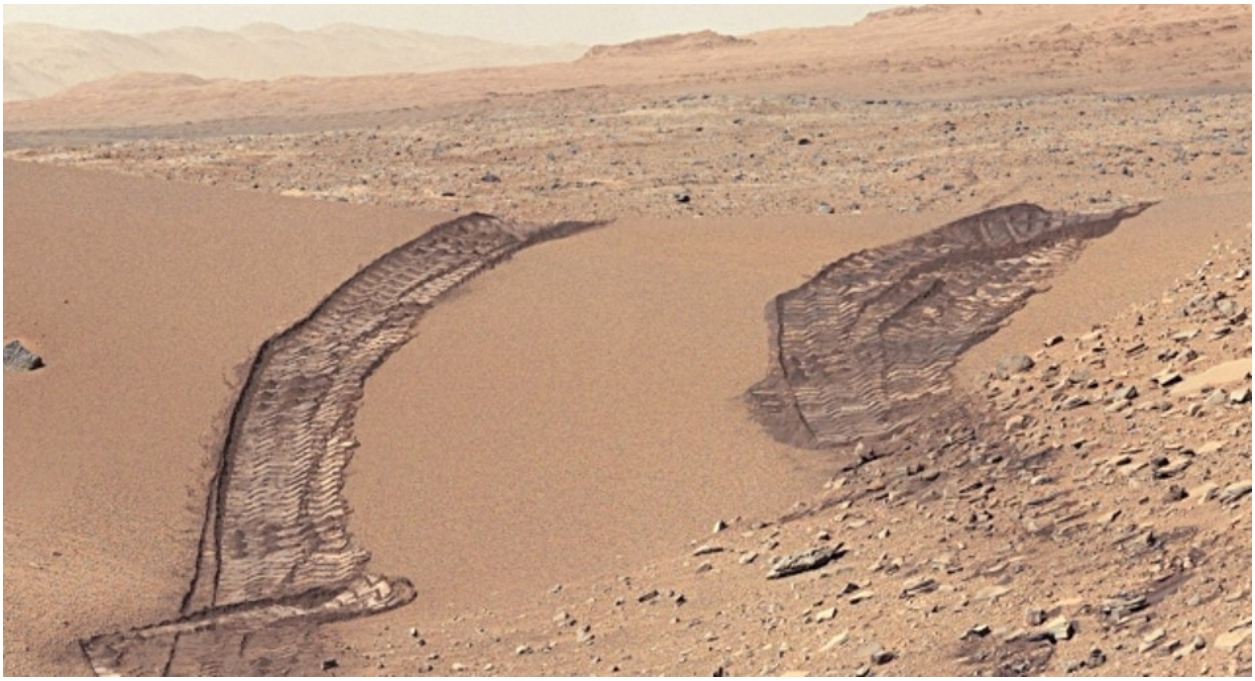

Figure 1.4: Curiosity's tracks on Mars driving up a steep slope and then back down [4]

In order to traverse this type of terrain successfully a mobility system must have high traction to insure it can climb steep sandy dunes and relatively low sinkage to insure the rover wont get stuck in deep sand [14]. This challenging terrain means the traction and sinkage affect where the rover can explore. The more area the robot can safely access, the more opportunity there is for science which is the main objective of most planetary exploration. These also affect how easily the robot can become entrapped. Entrapment often marks the end of a long and expensive mission and so it is avoided at all costs [15],[16]. While there are also rocky terrains on most planetary bodies, the loose granular soil is commonly the more difficult to traverse and thus the limiting factor in a rovers exploration. For these reasons a mobility systems traction and sinkage are key characteristics for a successful mission. Any improvement in this area can dramatically increase the amount of science that can be completed by planetary rovers because they can reach more difficult locations more quickly and without risking entrapment.

1.2 The Inching Method of Mobility

A new mobility system that has promise for planetary rovers is a wheeled rover that has a chassis that can change length allowing it to drive in a new way, by inching. This is accomplished in two stages, first the forward wheels drive forward, as the robot chassis expands, and the rear wheels stay put on the ground. Then when the chassis is fully expanded, the rear wheels drive forward, and the chassis contracts and the front wheels do not move. This is depicted in Figure 1.5. There

are two reasons this inching drive is being researched for planetary exploration applications. First, this system has been shown to perform extremely well in getting out of deep loose sand pits. The drawbar pull of the system, or the tractive ability of the robot, has also been shown to be higher than that of traditional mobility systems. Both these have been shown in previous work that is discussed further in Section 1.3.

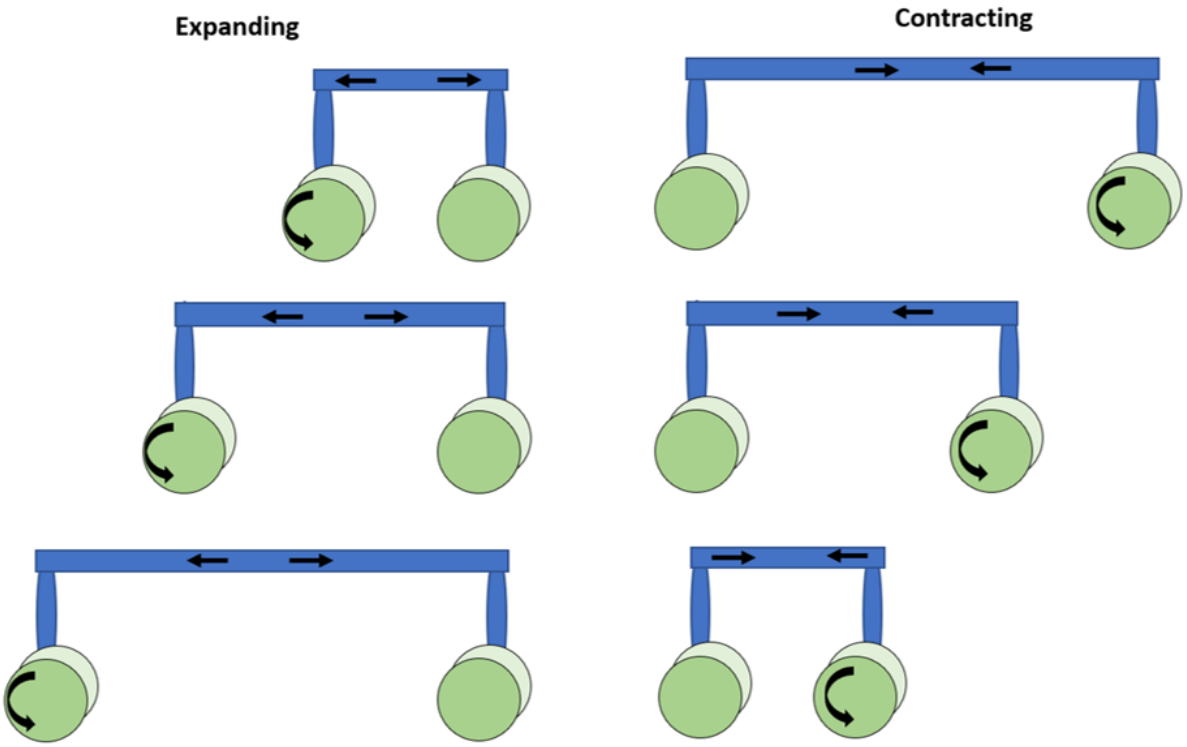

Figure 1.5: Inching overview, driving with two main cycles, expanding then contracting

1.3 Previous Work with Inching Mobility Performance

Inching has been studied in small amounts and has been shown to have beneficial characteristics for planetary exploration. In a few tests run on one robotic system that can perform an inching drive, the Scarab rover, it was shown that by inching the drawbar pull of the system was roughly doubled [5], [17]. These tests were run with a setup shown in Figure 1.6. The Scarab rover, pictured, was driven forward through sand as a cable held the vehicle back with a constant load. These tests therefore held drawbar pull constant and measured the slip with a positioning tracking system.

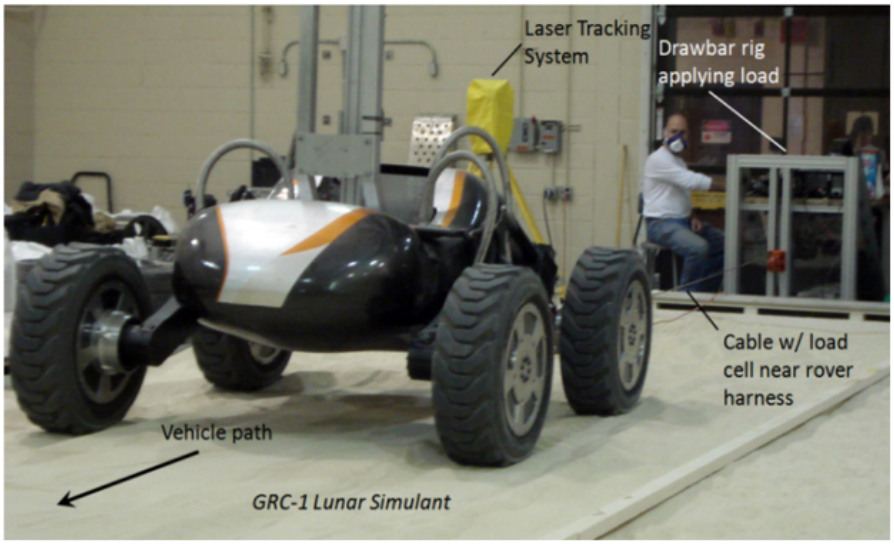

Figure 1.6: Test setup with scarab rover and cable to apply constant load [5]

Results from that study are shown below in Figure 1.7, where it is clear the inching is dramatically out performing the standard driving with respect to drawbar pull coefficient.

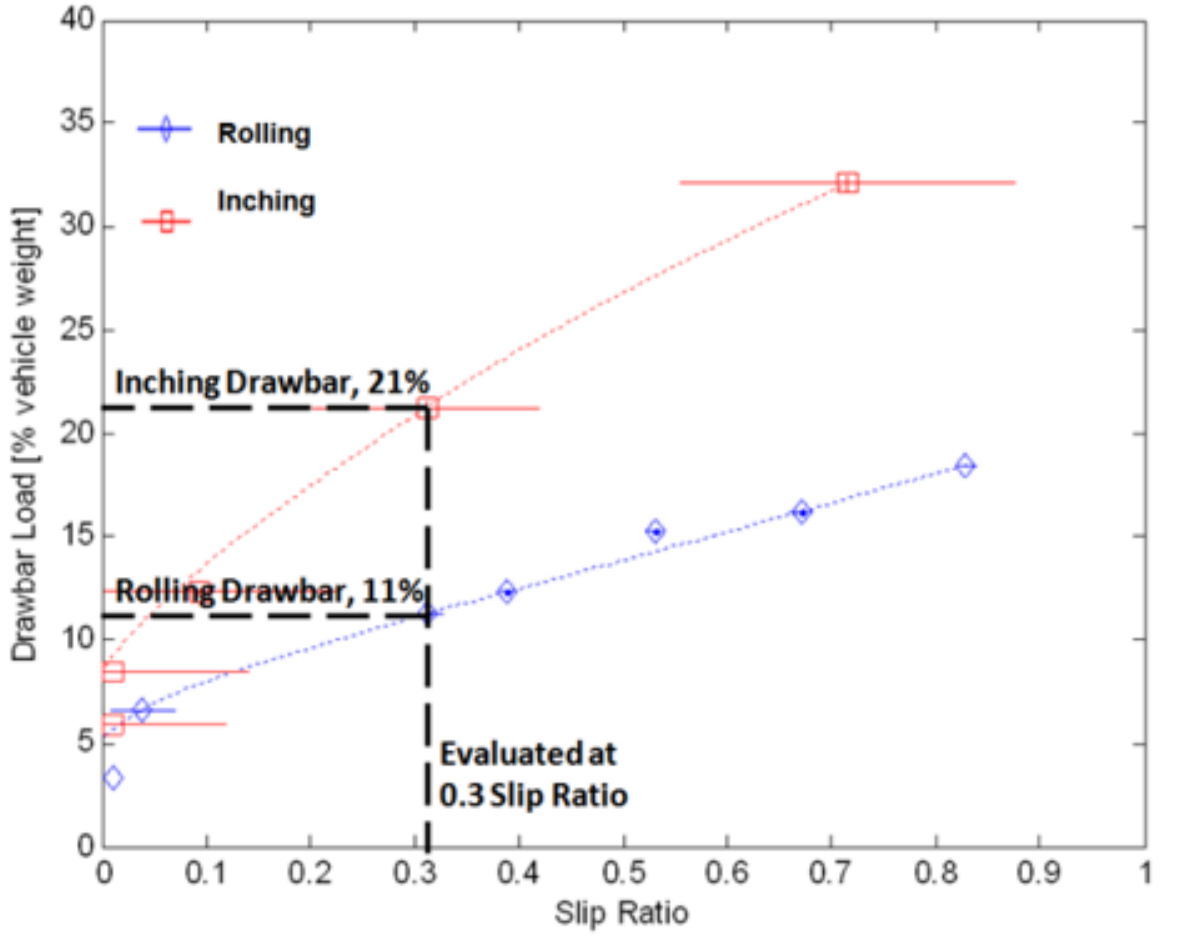

Figure 1.7: Results from inching tests performed with constant drawbar pull [5]

It was also shown on that same robotic platform that inching dramatically reduced sinkage in high sinkage material. When normal driving was used to traverse this material the velocity of the vehicle approached zero as the sinkage increased while when inching was used to traverse the material the forward velocity was constant and the sinkage was dramatically improved [6]. These test results are graphed in Figure 1.8

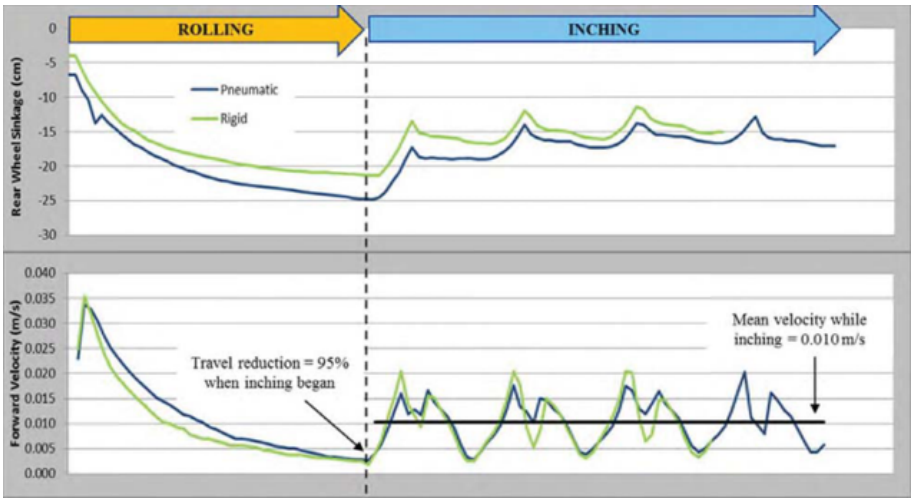

Figure 1.8: Results from tests performed where Scarab drove until stuck in sand and inches out of the situation [6]

For these reasons an inching mobility system appears to have many benefits and could be the next best drive system for planetary exploration. However, there is not enough data to have a full understanding of all the system parameters and their performance. This thesis attempts to fill that gap in the knowledge of an inching system.

1.4 Understanding Inching Parameters

This inching mobility system has many possible parameters that can be changed and coordinated. This thesis completes a full array of tests over all of these different parameters to understand how they affect the drawbar pull and sinkage of the system. These parameters are also combined in many tests to understand how they interact with each other. This full array of tests provides insight into how the different inching parameters affect the overall performance of an inching mobility system. The independent, dependent, and constant variables that will be tested are outlined in Figure 4.1, these variables are more fully defined in Section 3.5.

Independent Variables	Dependent Variables	Constant Variables
Wheel Speed	Drawbar Pull Coefficient	Vehicle Weight
Carriage Slip Percent	Sinkage	Wheel Design
Inching Percent		Sand Type and Preparation

Figure 1.9: Dependent, independent, and constant variables used for the study of inching

1.5 Thesis Statement

The inching mobility method is defined as driving with front and rear wheels rotating at different speeds while the distance between the front and rear wheels changes. The scope of this study is inching performed in loose granular soils with controlled slip values. This work aims to show:

Inching can improve drawbar pull performance compared to conventional methods of mobility when in conditions of high slip.

1.6 Contributions to Planetary Robotics

The contribution of this thesis is an extensive study of the different inching parameters and how they affect the traction and sinkage of a mobility system. These tests were completed using a novel two-wheel mechanism created for these tests. This study led to the understanding of which parameters were most effective in gaining traction and fully understanding how they can be changed to get different effects as needed.

Chapter 2

Planetary Rover Mobility Systems Background

This background will explore research occurring in the planetary rover mobility space, and how current mobility systems on Mars are used to explore the planet. The specifics of mobility performance are defined, and one testbed used to evaluate this performance is detailed. Single wheel performance was tested using this testbed revealing how and why some wheels perform better than others and generally how wheel performance changes with slip.

2.1 Rover Driving Techniques on Mars

Since Pathfinder landed on the surface of Mars in 1997 [18] NASA and JPL have always had a rover exploring the red planet. Over the years the design and complexity of these rovers has changed dramatically as technology improves. Understanding how rovers are driven and used on Mars is important to understanding how these mobility systems are used and what aspects are important to them.

Two of the more recent rovers, Spirit and Opportunity are twins, nearly identically hardware who explored two separate regions of Mars [19] [20]. They both landed in 2004, Spirit explored until 2010 and Opportunity explored until 2019.

These rovers are driven with three main types of commands, low level motor commands, directing driving primitives along a specific arc, line, or turn in place, and autonomous path selection [12]. Low level motor commands are used mostly for experiments using the wheels to dig and mobility system diagnosis and testing. Drive primitives are the fastest to execute as less time is spent gathering data and analyzing it with slow onboard computers, instead people do most of that work ahead of time with downloaded images from the rover. For this reason this drive mode is used whenever possible. Autonomous path selection was commonly used after a directed drive when the rover begins to drive on terrain that the rover drivers could not see when making the path plans

for the next day. In this mode the robot is given waypoints and can identify obstacles and select the best path to get from point A to point B. However this autonomous mode is much slower and is therefore not used except when it has to be. Lots of time goes into planning a rover path and keeping the rovers safe as they attempt to reach their goals. Any ability to make the mobility system designs inherently more capable and able to safely traverse more terrain means less time needs to be spent planning paths around impassable terrain.

Curiosity is the newest rover exploring Mars and it landed in 2012 and has been exploring the planet ever since [21]. Curiosity is much larger than Spirit and Opportunity but functions overall in very similar ways. The main drive modes are nearly identical to the previous rovers and most paths consist of arcs, turns, and lines generated for it by human rover planners. A new tool however was created to be used by the rover planners to help and automate the planning process [22]. This tool takes images from curiosity and automatically classifies them into five different potential terrain types. The software program then automatically generates paths between waypoints while keeping the wheels off sharp rocks. This allows the planning to be done on an efficient earth computer, the plan can be verified by humans and executed by the rover without wasting time planning automatically on Mars. This software is more advanced than the software for previous rovers but it is still attempting to solve a mobility problem with software instead of a better mobility system. If more terrain was easily passable, software would not be needed that could identify different terrains and spend time planning around them.

Driving on Mars can be a risky mission and extra time is always taken to insure the safety of the mission. The mission must plan based on how its mobility system performs and what dangers could entrap the rover forever. A more capable mobility system would allow more focus to be on the science of the mission and less time could be dedicated to insuring the safe passage of the rover.

2.2 Current Planetary Rover Mobility Research

In the development of rovers to explore planetary bodies, specifically Mars, many new mobility system designs have been developed and tested to attempt to get better performance. Often these systems are mass, and volume constrained to fit within a certain launch or decent vehicle.

The European Space Agency (ESA) worked to develop a better mobility system for their ExoMars rover mission [23]. They studied various suspension methods to get a statically stable system in any direction up to 40 degrees that could also easily negotiate around obstacles and climb the necessary slopes. They also attempted to understand the effects of various solid and compliant wheels on the traction abilities and motor torque requirements. However, this comprehensive study resulted in a mobility system that closely resembled the existing Mars Exploration Rover (MER) rover except for the change from solid to compliant wheels.

After this study there has been a push by a few National Aeronautics and Space Agency (NASA) centers to develop and understand unconventional mobility system. Johnson Space Center devel-

oped a lunar transport prototype vehicle called Chariot, Figure 2.1 [7]. This vehicle has a six wheeled mobility system with passive and active suspension. Each wheel module can raise or lower itself using a separate motor, allowing the vehicle to lower itself for crew loading and to raise itself for obstacle avoidance. While this motion does not enable inching, it is a glimpse into some of the new, more advanced driving NASA is experimenting with.

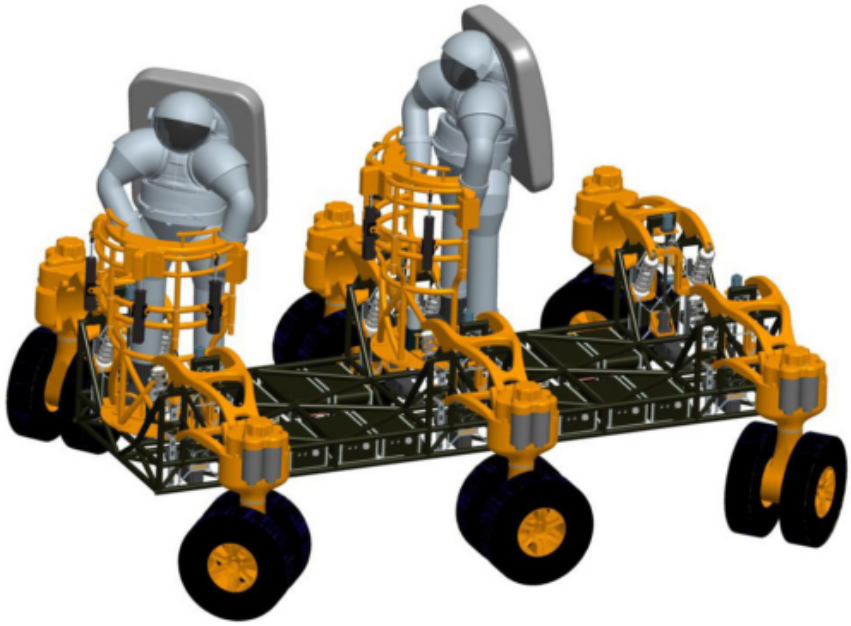

Figure 2.1: Chariot rover designed at NASA Johnson Space Center [7]

NASAs Jet Propulsion Laboratory (JPL) also developed a highly unconventional mobility platform ATHLETE: the All-Terrain Hex-Limbed Extra-Terrestrial Explorer, Figure 2.2 [8]. This rover has six wheels that are all attached to multi- degree-of-freedom limbs. This allows the rover to walk out of sand if it is ever stuck and climb up steps that would not be possible with traditional mobility systems. This robot would be capable of inching if a controller was built to enable it, however it was not designed for this purpose. It would also be capable of doing more of a walking type of mobility.

Figure 2.2: Athlete rover designed at JPL [8]

The rover Scarab, Figure 2.3, was also designed with a unique four wheeled mobility system that can change how far apart its' front and rear wheels are [9]. This allows the robot to stay level on varied terrain and slopes and allows it to change clearance height for drilling purposes. This allows Scarab to drive by inching and research was completed using scarab to study inching. This is explained in further detail in Section 1.3.

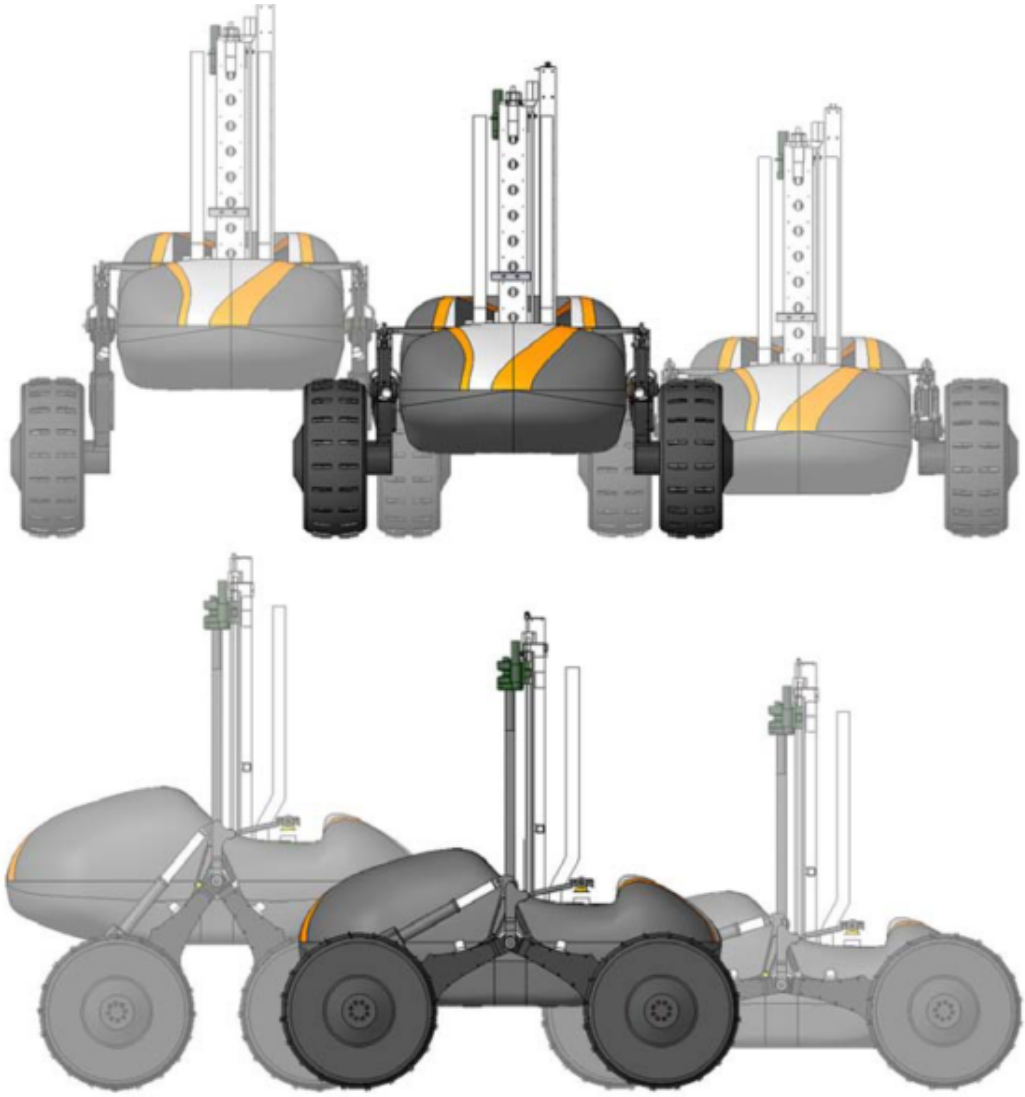

Figure 2.3: Scarab rover designed at Carnegie Mellon University [9]

Mobility systems of many shapes and forms are being studied for planetary rovers to gain even a little bit of performance without compromising on size and weight.

2.3 How to Define Mobility Performance

A key function of any planetary rover is its' mobility performance. A rover must be able to traverse the planet with a minimal fear of being entrapped, stuck on obstacles, or unable to climb slopes. Terramechanics, the study of wheel soil interaction, plays a large role in the development of planetary rovers as it governs how well any mobility system can traverse its surrounding [24].

Knowing how wheels interact with soil provide insights into the design of rovers and also provide important simulation insights and allow rover drivers to more accurately control the rover. The understanding of wheel-soil interaction is especially important to planetary robotics to understand what hills a rover can climb. Understanding how wheels interact with soil gives insights into how the wheels will perform when attempting to get enough traction in the soil to climb a hill [25] [26]. Terramechanics definitions and terms commonly used when discussing planetary rover mobility systems are drawbar pull, wheel slip ratio, and sinkage.

One important factor in mobility system performance for planetary rovers is its net traction, or drawbar pull. This is equivalent to the thrust generated minus any motion resistance forces. The calculation for drawbar pull is shown in Equation 2.1, where DP is the drawbar pull, H is thrust and R is the sum of motion resistances [27] [28].

$$DP = H - R \tag{2.1}$$

Drawbar pull is commonly normalized by vehicle weight (or wheel payload) in order to compare wheel performance consistently. This form is called drawbar coefficient [29] and can be calculated using Equation 2.2, where W is the vehicle that each wheel is holding. An increase in drawbar pull coefficient is equivalent to a robot being able to pull a heavier trailer behind it or a robot being able to climb a steeper hill. Drawbar pull coefficient is therefore a very important metric for rover mobility performance.

$$DP_{coef} = \frac{DP}{W} \tag{2.2}$$

A term that is closely related to drawbar pull coefficient is wheel slip. Wheel slip is defined using the slip ratio and it is the ratio between the linear velocity calculated using the wheel angular velocity and radius, and the actual linear velocity achieved. This definition is written out in Equation 2.3.

$$Slip_{\%} = (\frac{w * R}{V} - 1) * 100 \tag{2.3}$$

Wheel slip has been shown to increase the drawbar pull of a mobility system making it key to how rovers are able to climb slops. The slip of a wheel is directly related to how steep of a hill cam be climbed, an example graph of slope versus slip for one mobility system can be seen in Figure 2.4.

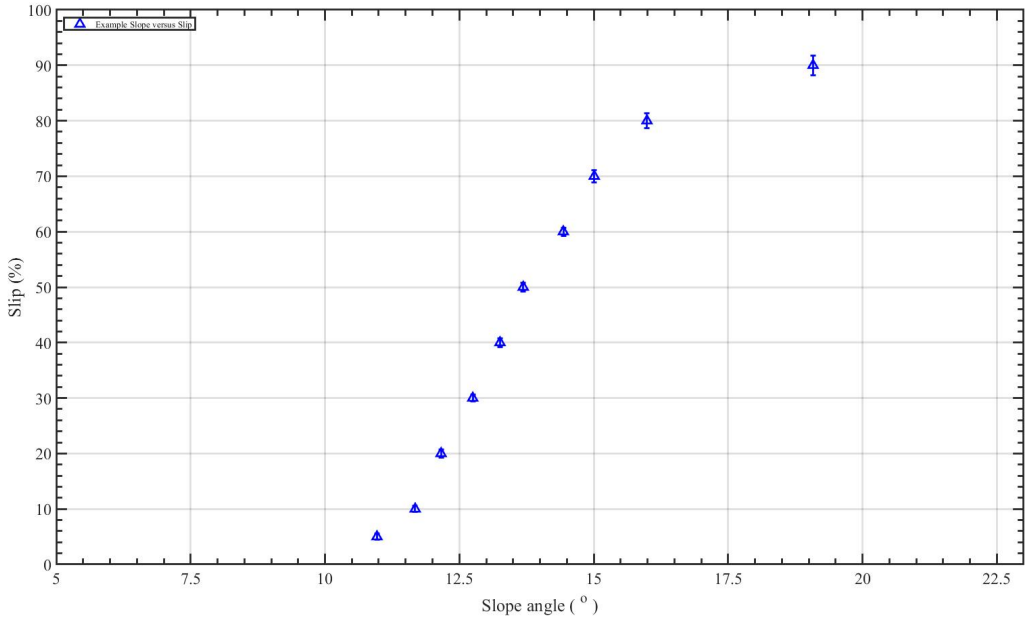

Figure 2.4: Example plot of slope versus slip

Another factor that is important to a mobility system performance is the sinkage while traversing loose soil. If the sinkage of a vehicle becomes too high, a vehicle risks becoming entrapped and stuck in the soil. However, it has been shown that mobility systems get increased drawbar pull as the wheel slip approaches 20% and above 20% there is no increased drawbar pull advantage [17]. To achieve 20% slip more sinkage will naturally occur and therefore some level of sinkage is beneficial to mobility systems while too much sinkage is detrimental.

2.4 Testbed used to Analyze Mobility Performance

One studied aspect of mobility systems is their wheels, as improving wheel performance can easily improve overall mobility system performance. Many different testbeds are used to study planetary wheel performance. A single wheel testbed was used in [25] to explore wheel drawbar pull and slope climbing ability of wheels. A similar testbed was used in [30] to compare wheel performance in a testbed to predicted performance in a simulation.

One such testbed was re-purposed for the work of this thesis and as such a description of the initial testbed is provided below.

The testbed is a 1.54 meter wide by 3.67 meter long tub and all the tests were run with it filled with Soil Direct #90 sand. This soil was selected for Mars 2020 Rover wheel testing. It was selected based on median particle size and particle shape. This soil was also required to be well sorted,

meaning the range in particle size is low. This soil was considered a bounding test scenario for slope climbing situations on Mars. The testbed consisted of a driven motor where a wheel would be attached that is connected to a driven carriage that drives back and forth down the length of the testbed. By driving the wheel and the carriage at synchronized rates the slip of the wheel in the sand can be controlled entirely to test how it performs at various slip values. The carriage motor can also easily be disengaged so that tests can be run fully self-propelled by the wheel driven motor. The motor is connected to the driven carriage by a 6-axis load cell that is used to measure all forces and torques between the wheel and the carriage. Using this load cell the drawbar pull can be assessed at different slip values to characterize the performance of different wheels under the same load and conditions. The wheel and load cell can also freely translate up and down so the wheel will naturally sink into the soil under a load as it drives down the testbed. This allows the sinkage to also be measured and used as a possible performance metric. Figure 2.5 is a diagram of the sand testbed and its various components. A picture of the actual testbed is shown in Figure 2.6.

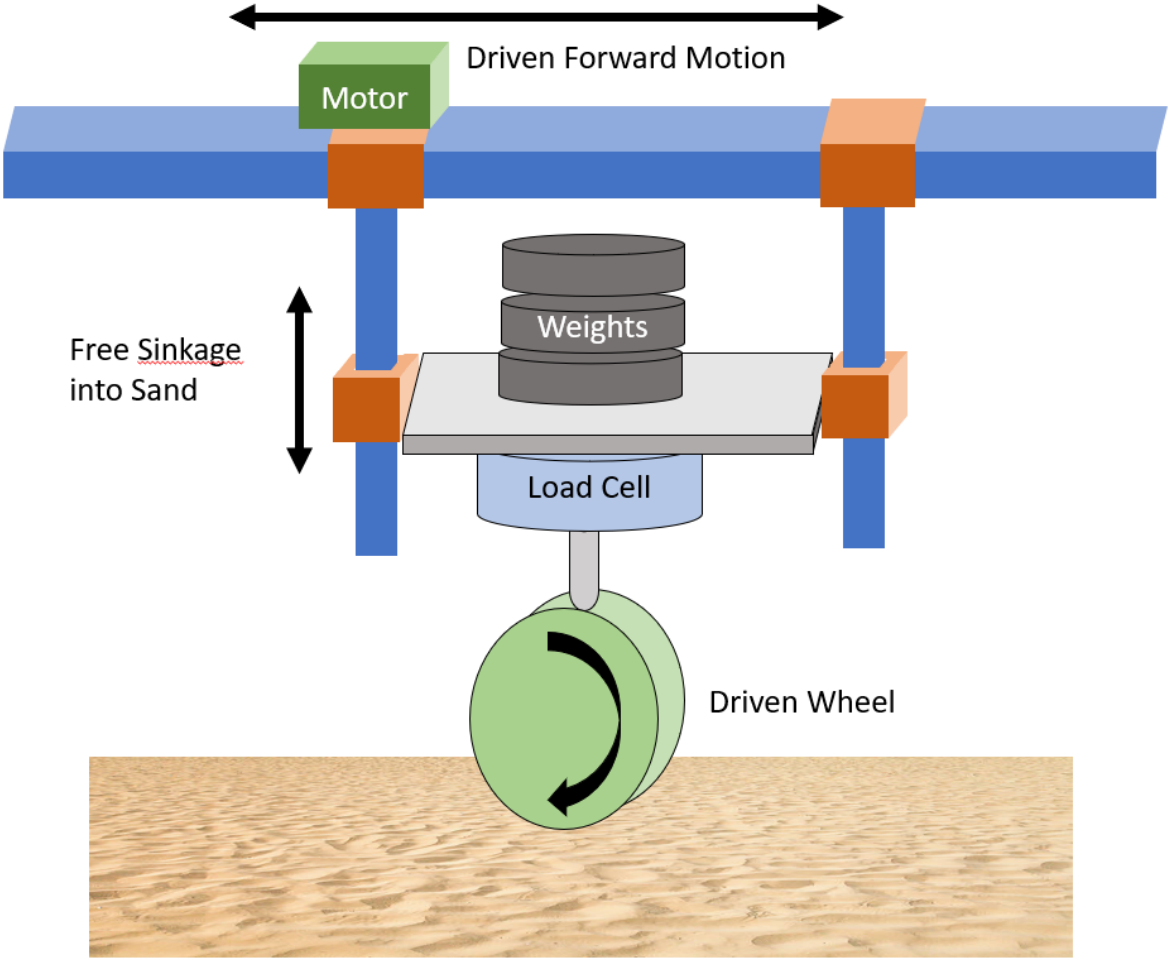

Figure 2.5: Single wheel testbed diagram

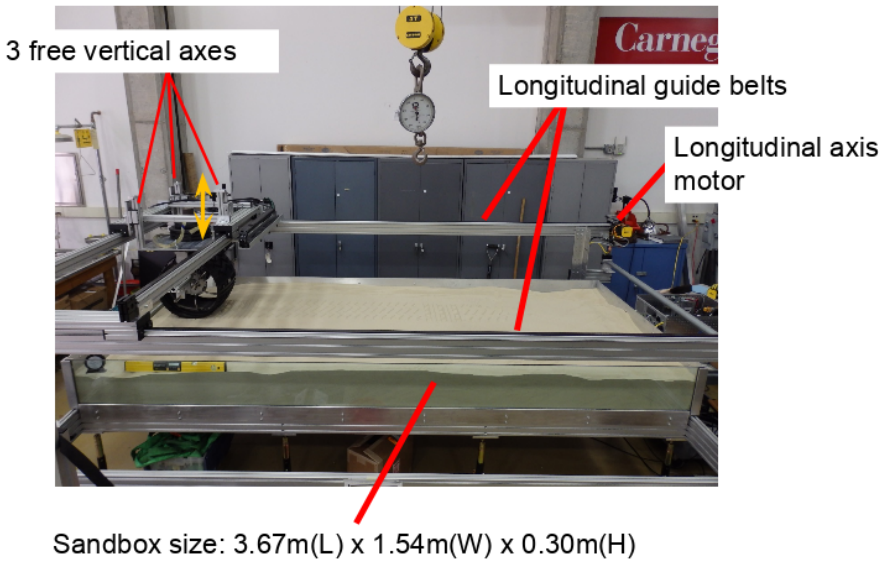

Figure 2.6: Single wheel testbed

The testbed is run with a connecting computer running a custom software program. This program was built with a UI (User Interface) that allows the testbed operator to input various test parameters, get biases from the load cell before each test, run tests and watch the live data being collected, and post process the data to build useful graphs and charts. When a test is run the software then takes all the users input and builds code to send to the motor controller to execute the test. While the test is being executed the software collects all sensor data and publishes it to a SQL database on the local computer. This is the data that is later queried to build the post processed graphs and charts.

2.5 Single Wheel Performance in Sand Testbed

Tests run in the single wheel testbed in previous work provided new and more advanced insights into wheel performance in loose soil. These tests helped to increase the understanding of how the soil behaved underneath such wheels and how that leads to wheel performance.

Single wheels when tested in sand show a linear drawbar pull coefficient increase as slip increases from 0% - 20%. Then as slip increases past 20% the drawbar pull continues to increase but much slower[17]. This is shown as a graph in Figure 2.7.

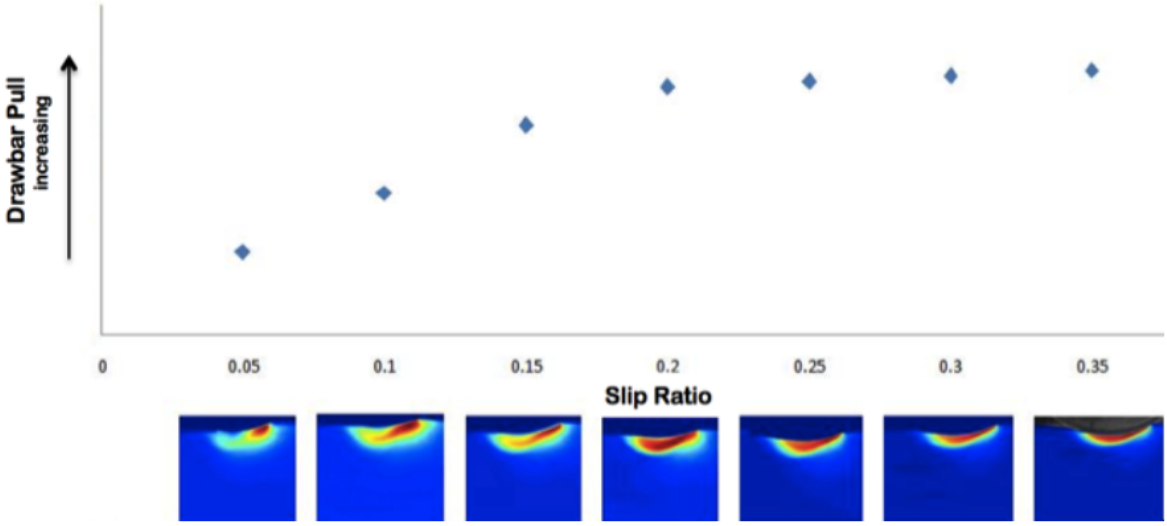

Figure 2.7: Single wheel drawbar pull versus slip

Shown in images below each slip value in Figure 2.7 are results from sub-surface soil imaging as tests were completed. These tests show at the 20% slip point the soil shear behavior changes dramatically and is pushed backwards considerably more instead of being pushed forward as it is at low slips [17]. This soil behavior was shown to correlate directly with drawbar pull, making the sub surface soil behavior critical to optimal wheel performance.

Grousers were also tested to determine how they affect single wheel performance [22]. It was determined the main effect of grousers is sweeping soil from in front of the wheel so that the sub surface soil is all moving backwards and not forwards. Given this there is a minimum grouser height and spacing that will catch soil before the wheel makes contact with it. As long as at least this many grousers are used, wheel performance will be optimized.

2.6 Summary

While current mobility systems on Planetary rovers do perform their jobs and allow the rovers to explore their planets, lots of time and energy goes into avoiding obstacles, and keeping the rovers safe from hard to navigate terrain. Software solutions are slowly starting to make this job easier and faster, but having a more robust, better performing mobility system would also reduce the time required to avoid obstacles because fewer terrains would be classified as obstacles. For these reasons NASA is constantly trying to develop and test new mobility systems to help explore other planets faster and easier.

In order to test and determine how mobility systems perform compared to each other they are tested and evaluated. They must be able to produce enough drawbar pull to climb slopes and they must

not sink so much as to become entrapped in deep soil. Wheel performance was another important aspect to study as wheels could easily improve overall mobility performance. These wheels were compared and studied using a single wheel testbed. Results from these tests show that as wheel slip increases from 0% to 20% the resulting drawbar pull produced increases linearly, then beyond 20% the drawbar pull produced levels off considerably and only increases slightly with increased slip. These tests provide the expected trends to be observed with inching as it is tested at increasing large slip values.

Chapter 3

Inching Mobility System Testing Setup

To gain a better understanding of inching, a test setup was needed to run tests and gather data about the performance of inching. Past research has consisted of a few tests, with no concentrated effort to fully understand how and why inching outperforms traditional driving. To collect all this data a testbed was needed with a mechanism that could inch in many different ways. The testbed also needed to be able to perform consistent repeatable tests, and gather all the data required to analyze the performance of each test.

3.1 Two-Wheel Mechanism used to Test Inching

The two values desired to properly characterize an inching mechanisms performance are its sinkage and drawbar pull coefficient. Since the already existing sand testbed described in Section 2.4 has the capability of measuring performance metrics this testbed was slightly modified and used to run a wide range of inching tests. A diagram of the testbed, including its physical modifications can be seen below in Figure 3.1.

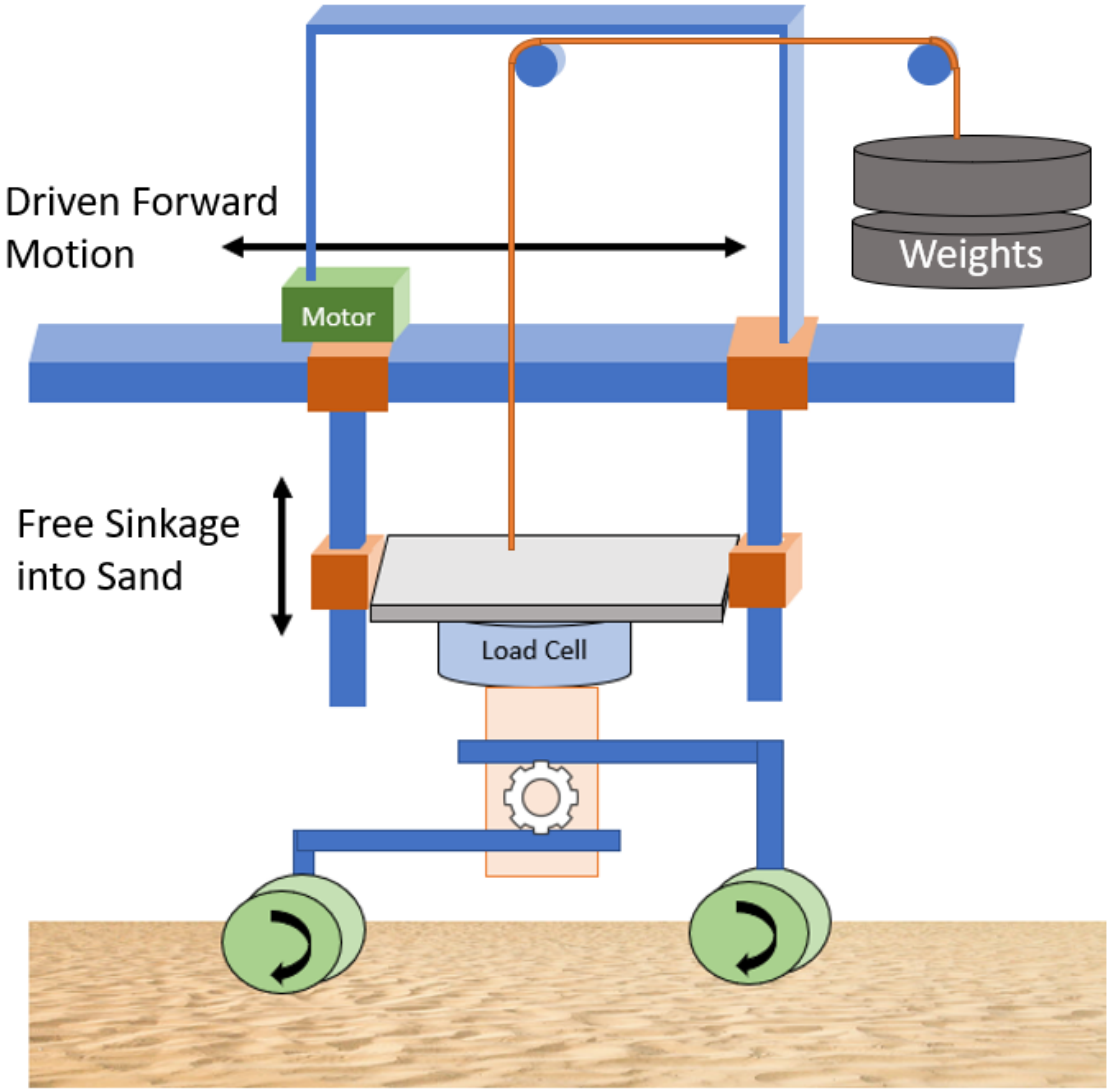

Figure 3.1: Two-wheel testbed

The biggest modification was a two-wheel mechanism mounted below the load cell in the place of the motor and one wheel. This load cell and two-wheel mechanism can still freely translate up and down to measure overall sinkage values. The two-wheel mechanism has two individually driven wheels with their own motors so they can be controlled separately. These two wheels are connected with linear slides that are actuated. This allows the distance between the wheels to be controlled by driving a rack and pinion system. With this setup various types of inching and driving through the sand are performed while recording the performance of the system. Figure 3.2 shows a picture of the two-wheel testbed and the load cell connected to the vertically translating portion

of the testbed.

The added two-wheel mechanism has two racks, one connected to each wheel, and one central pinion to drive the wheels together and apart at equal speeds. Once the pinion is set in the middle of the two wheels, it will always stay perfectly in between them and will always drive them together and apart at the same speed. The pinion is underneath an aluminum and plastic box seen in the middle of Figure 3.2. This block mounts to the center support and allows the two racks to slide within it, holding both racks mesh with the pinion even when the structure is loaded with weight. Two linear bearings are also used, again one attached to each wheel mount that help transfer forces and slide between the central support and each wheel mount. Two limit switches are used above the central pinion to detect when the outermost and innermost positions have been reached. They are attached to the yellow plastic in Figure 3.2 on the center mount. The innermost position was defined by how close the wheels could be to each other without risk of hitting, and the outermost position was defined by keeping both racks well within their support structure on the opposite wheel mount (this is the black box seen in Figure 3.2 above the right wheel).

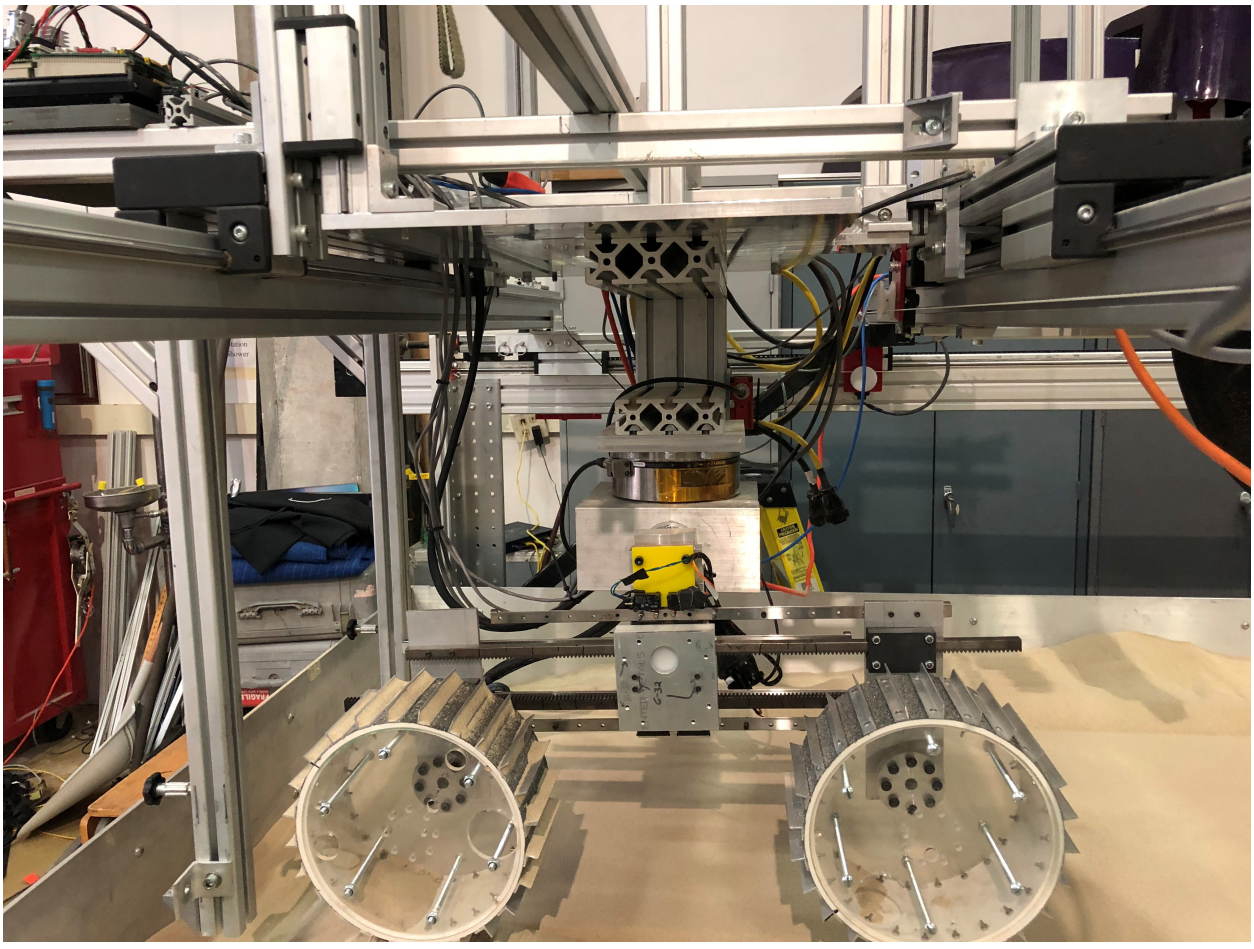

Figure 3.2: Two-wheel testbed connected to load cell

Two identical wheels were used on the two-wheel mechanism. They are 22 cm in diameter, 11.5 cm wide, and each have 24 grousers that are half an inch long. The grouser height and spacing for the wheels was chosen using the grouser equation in Ref [22], also shown below in Equation 3.1. ϕ is the angular spacing, i is the slip value, $\hat{h}$ is the normalized grouser length, and $\hat{z}$ is the normalized sinkage. For this equation, a slip of 20% was desired as that was found in, Ref [17], to produce optimal drawbar pull with single wheel tests. A sinkage of 10mm was used as that is about 5% of the wheel diameter which seemed like a good nominal sinkage value to use. Using these factors and the overall size of the wheels it was determined that the angular grouser spacing was 0.28 radians or 16 degrees which equates to approximately 24 grousers needed on each wheel. All the tests were run using these identical wheels.

$$\phi \leq \frac{1}{1-i} * (\sqrt{(1+\hat{h})^2 - (1-\hat{z})^2} - \sqrt{(1-\hat{z})^2}) \tag{3.1}$$

The structure that was previously designed to support the vertical sliding on the carriage was designed to be very robust, so it ended up being heavy. The linear rail supports and overall structural design of the two-wheel carriage was not designed to support such high loads. Therefore a counter weight system was also added to the testbed to offload much of the weight that was loading up the two-wheel mechanism. 70 lbs. were hung off the front of the carriage pulling up on the vertical structure. This resulted in only 24kg on the two-wheel mechanism. This allowed the mechanism to not bow and bend as tests were run. This is also a much more reasonable load relative to the size of the wheels and the size of robot that such wheels would likely be carrying. This counterweight, and structure designed to support it can be seen in Figure 3.3, the actual weights are hanging off the front in the right of the image.

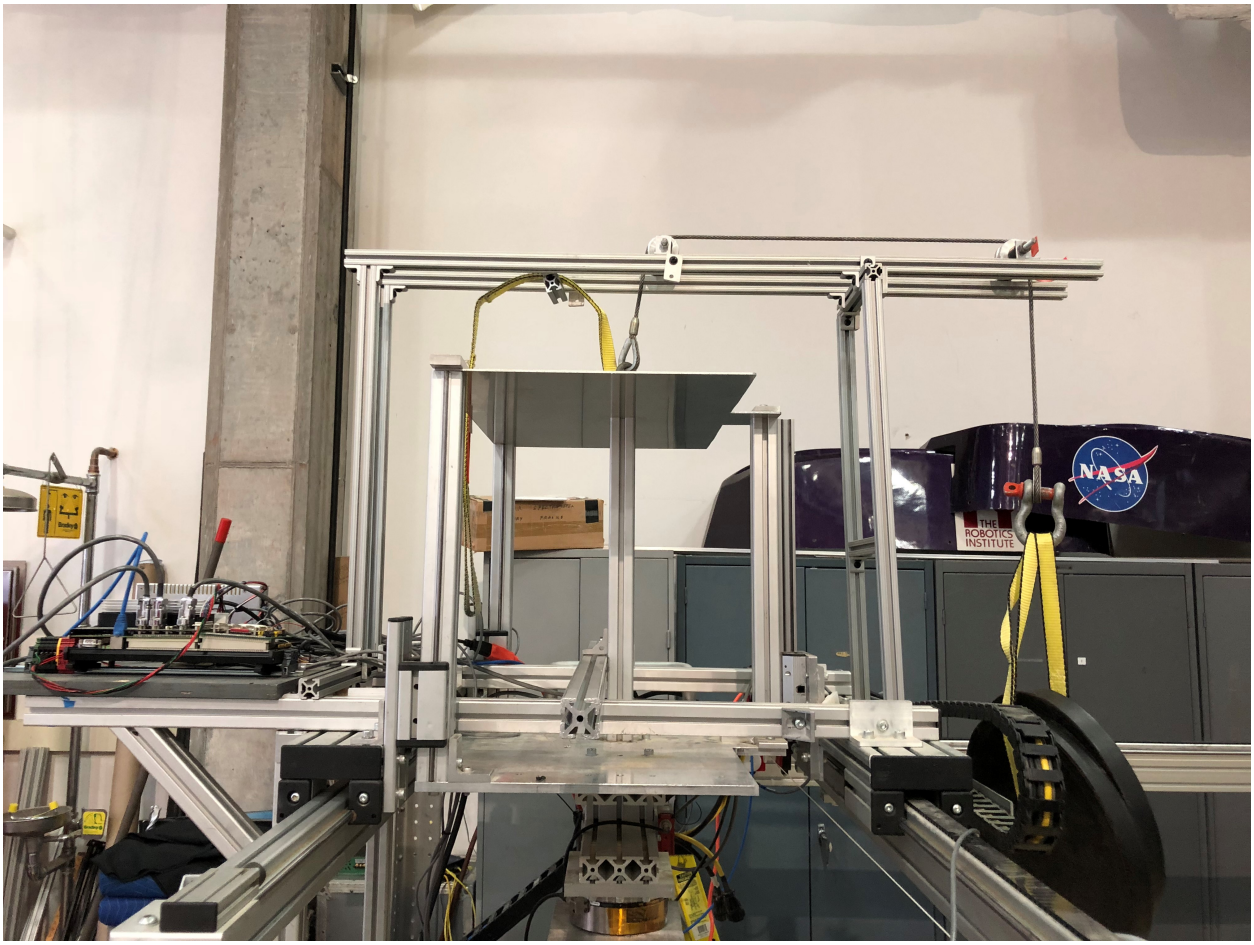

Figure 3.3: Two-wheel testbed counterweight

3.2 Testbed Software Updates

New software was written to interface with and run the testbed that was added below the force torque sensor. A lack of motor ports in the original motor controller forced the use of a secondary, new motor controller to run the motors on the two-wheel mechanism. Software already existed to setup and run tests with the original testbed, and it was modified and updated to include the new features. One of the biggest changes was communication between the two different motor controllers. On the new motor controller software was written for that controller that gets uploaded and executed when a test is started. This software has two main loops, expanding, and contracting. The software toggles between these two loops as limit switches are hit and continues until stop code is uploaded to the controller at the end of the test. Another big change is how the data coming from both motor controllers is logged and stored in the testbed database. Data is synchronized between both motor controllers before it is stored in the database. Finally, new settings were added to allow

for the various types and inching and tests that would be run, and small changes in functionality were added to account for these changes and additions.

3.3 Testbed Calibration

To run many of the inching tests, four different motors had to be in sync to assure the desired slip parameters were maintained. The two wheels had to be driven at their desired angular speed. The linear expansion had to perform at the right linear speed. And the carriage had to move forward at the correct linear speed. All these speeds were controlled with the testbed software and were driven by encoder ticks per second. To properly tune the encoder ticks per second to desired linear speed encoder ticks per rotation, accurate wheel radius, accurate pinion radius, and gear reductions were all needed. Once all these values were input in the software, they were all tested to verify the proper speeds were obtained. The wheels were marked at the rim and then driven at a slow desired speed while suspended in the air. The time was measured it took to rotate once with a stopwatch three times to verify the desired speed matched the driven speed. Similar tests were performed with driving the carriage a long distance at a slow speed and expanding the two wheels a given distance at a set speed. The input measured parameters were adjusted slightly until the measured and desired speeds of each individual piece of the system were perfectly coordinated.

3.4 Testbed Data Storage

As tests are run, a large amount of data is stored in a database from various pieces and sensors in the testbed. From both motor controllers, the speed, and current of all motors were collected. A string potentiometer attached to the vertical and stationary parts of the carriage collects sinkage data. A laser range finder pointing down at the flat sand also collects sinkage data. The six-axis load cell collects and stores all three forces, and all three torque values throughout each test run.

3.5 Inching Parameters to Investigate Using Testbed

For this method of mobility a few parameters need to be defined to fully describe the inching motion. Wheel slip ratio is a commonly used parameter defined in Section 2.3, but with this two-wheel mechanism there are two different wheels with two different slips. These wheel slips are controlled indirectly through a combination of the carriage speed, the mechanism expansion speed, and the wheel angular velocities. As such, the addition of this wheel expansion speed parameter required new definitions to be made.

The four main commanded velocities are the carriage velocity, the expansion velocity, the angular velocity of the slower wheel (usually zero), and the angular velocity of the faster wheel. Since

slip ratio is defined as the ratio between actual linear velocity and linear velocity resulting from the angular velocity, commanded wheel velocities will be defined as their commanded linear velocities. These velocities are define in Equations 3.2 and 3.3). Figure 5.11 contains a diagram of the two-wheel mechanism with labels for all the commanded velocities.

$$V_{slw} = r_{wheel} * \omega_{slw} \tag{3.2}$$

$$V_{fst} = r_{wheel} * \omega_{fst} \tag{3.3}$$

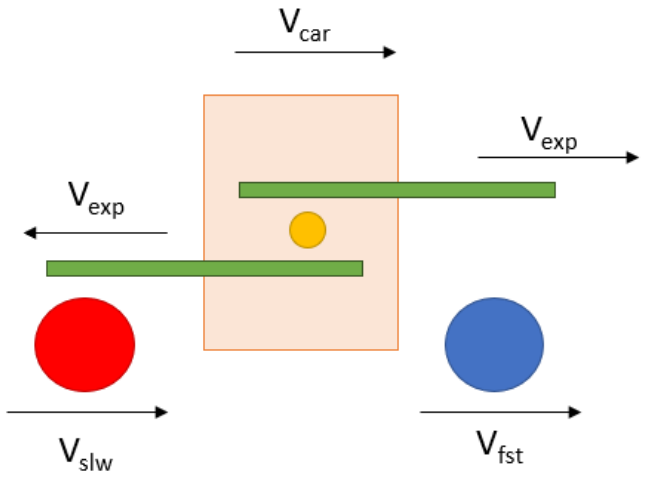

Figure 3.4: Two-wheel mechanism velocities

The first parameter to be defined is the carriage slip percent. This will be defined similarly to wheel slip, and will be the ratio of the actual commanded carriage speed relative to what the carriage speed would be with no wheel slip at the given wheel velocities. This is equivalent to thinking about the overall slip of an entire vehicle, how much fowrard progress the vehicle is making relative to how much forward progress it should be making if the wheels weren't slipping at all. Using this definition, the driven carriage speed can be calculated using Equation 3.4, given the fast and slow wheel velocities and the desired carriage slip percentage.

$$V_{car} = (\frac{V_{fst} - V_{slw}}{2} + V_{slw}) * (1 - car_{\%}) \tag{3.4}$$

The second parameter to be defined is the inching percent. Similarly, to carriage percent the speed of the inching expansion can be varied relative to what the nominal speed should be. Nominally, when performing perfect inching, the mechanism should expand at a rate of half the difference

between the two-wheel speeds. This state of perfect inching will be defined with an inching percent of 100%, and is equivalent to the expansion speed being perfectly synchronized with the wheel speeds. By multiplying half the wheel speed difference by the desired inching percent, the corresponding expansion rate can be calculated using Equation 3.5.

$$V_{exp} = \frac{(V_{fst} - V_{slw}) * inc_{\%}}{2} \tag{3.5}$$

Table 3.5 shows various example input percentages and linear wheel velocities and the resulting expansion and carriage velocities. With 100% inching and 0% carriage slip the expansion speed is just half the difference between the wheel velocities. The carriage speed is also half the difference in wheel speeds plus the slowest wheel speed, which is zero in this example. As inching percent is increased, the expansion speed increases proportionally and as the carriage slip increases the carriage speed decreases proportionally.

Inching Percent ($inc_{\%}$)	Carriage Slip ($car_{\%}$)	Slow Wheel Speed (V_{slw}) cm/s	Fast Wheel Speed (V_{fst}) cm/s	Expansion Speed (V_{exp}) cm/s	Carriage Speed(V_{car}) cm/s
1	0	0	2	1	1
1.5	0	0	2	1.5	1
0.8	0.4	0	2	0.8	0.6
1	0	1	3	1	2
1.2	0.1	1	3	1.2	1.8

Figure 3.5: Example velocities for various parameters

Throughout all the tests run, parameters are held constant or varied to understand their role in the overall performance. These parameters include fast wheel velocity, slow wheel velocity, carriage slip percentage, and inching percentage.

3.6 Summary

A single wheel testbed was updated to include a two-wheel mechanism capable of inching. This mechanism has three controllable motors, two wheels, and the expansion motor controlling the distance between the wheels. Software was updated to control and store data about this new two-wheel mechanism, and all the new motors were calibrated to be in sync. Finally new parameters were defined to explain the motion of this inching device. The carriage slip percentage will be defined similarly to the slip percentage of the whole vehicle. The inching percentage is the speed of the expanding motor relative to the difference in wheel speeds, with 100% meaning the expansion speed is perfectly synced with the wheel speeds.

Chapter 4

Inching Tests Performed

Tests were run with the independent, dependent, and constant variables shown in Figure 4.1. The test campaigns were setup to test how wheel speed, carriage slip percent, and inching percent all affect performance. The two performance metrics used and studied are drawbar pull coefficient, or how much traction and towing ability the system would have, and sinkage. Throughout the tests, weight added to the vehicle was held constant. The wheel design itself was not studied and was held constant. The sand type was never changed and was also a constant.

Independent Variables	Dependent Variables	Constant Variables
Wheel Speed	Drawbar Pull Coefficient	Vehicle Weight
Carriage Slip Percent	Sinkage	Wheel Design
Inching Percent		Sand Type and Preparation

Figure 4.1: Dependent, independent, and constant variables used for the study of inching

Five main test campaigns were run, each with their own objective. The first set of tests were baseline tests, where no inching was done and the performance of the testbed is characterized at a range of carriage slip percentages, defined in section 3.5. These tests characterize how the wheels, and the testbed itself perform when driving normally with two wheels. This test campaign also includes tests to determine if absolute wheel speed affects performance. These tests will all act as a baseline for the following tests and will allow inching to be compared to normal driving.

The second test campaign investigates how perfect inching performs in the testbed. Perfect inching will be defined as the expansion speed being perfectly in sync with the wheel speeds, also equivalent to 100% Inching Percent. These tests are all run with one wheel not turning, at a variety of

slip percentages. Again, this study attempts to understand if absolute wheel speed affects performance. These tests most closely represent previous work done with inching and are run to confirm previous inching study results described in Section 1.3.

The third test campaign includes tests where perfect inching is again performed but both wheels are driven, one is just driven faster than the other. Inching, as it has been studied in the past, has always been with one wheel not turning, however this is not a fundamental requirement of inching. This type of inching was studied because if both wheels keep driving a robot could potentially cover more ground faster which would be a benefit. However, this speed will likely come at the cost of drawbar pull as not having one planted wheel in the soil should result in a lower drawbar pull coefficient.

The fourth test campaign investigates the effects of varying the inching percent away from 100%, which is defined in Section 3.5. These tests vary the speed that the chassis length is expanded and contracted relative to the wheel speeds, also known as the inching percent. Along with carriage slip percentage, this is another parameter than can be varied and can affect the wheel slip and therefore the performance, therefore it will be interesting to also study the effects of this final degree of freedom in the system.

The fifth, and final, set of tests is again performed with no inching while varying the speed of the two wheels. This is to begin to understand if some performance can be gained without inching but just with some form of traction control.

4.1 Description of Specific Tests Run

Overall a total of 120 individual tests were run. Since tests were run in triplicate 40 unique combinations of parameters were tested. Wheel speeds were all between 1 cm/s and 3 cm/s. These speeds were chosen as they are close to the speeds a real planetary rover of this size would be driven, based on speeds and sizes of actual Mars rovers defined in [12], [31], [11], [13].

4.1.1 Baseline Mobility Tests

Eight different baseline tests were run with no inching and both wheels driven at the same speeds. At 0% and 60% carriage slip the tests were run at slower and faster wheel speeds. These tests produced no difference in performance so tests were run at a single speed for the remaining slip values between 0% and 60%. The tests run are marked with Xs in Table 4.2.

Inching % = 0 for all tests			Wheel Speeds	
			1 (cm/s)	0.5 (cm/s)
Basic Two Wheels At Same Speed	Carriage Slip %	Self Propelled	X	
		0%	X	X
		10%	X	
		20%	X	
		40%	X	
		60%	X	X

Figure 4.2: Baseline tests performed

4.1.2 Inching with 100% Inching Percent Tests

Thirteen tests were run all with an inching percent of 100%, also known as perfect inching. All these 100%, perfect inching tests are outlined in Table 4.3. This includes tests of the perfect inching with one wheel not rotating along with tests of the perfect inching with both wheels always rotating.

Inching % = 100 for all tests			Wheel Speed Slow:Fast(cm /s)		
			0 : 1	0 : 2	1 : 3
Perfect Inching Two Wheels at various speeds	Carriage Slip %	Self Propelled		X	
		0%	X	X	X
		10%		X	X
		20%		X	X
		40%		X	X
		60%	X	X	X

Figure 4.3: 100% inching tests performed

Inching with One Wheel Not Rotating

Similarly to the baseline tests, tests were run with one static wheel and two different fast wheel speeds at the high and low carriage slip value to rule out wheel speed as a contributing factor to performance. Once this was done, all the carriage slip values were tested at just one fast wheel speed with the slow wheel speed being zero. These tests were designed to compare baseline performance to perfect inching performance similarly to inching tests performed in previous work outlined in Section 1.3.

Inching with Both Wheels Rotating

A second set of tests was run at every carriage slip value with a slow wheel speed not equal to one. These tests were designed to investigate the effects of having one completely stationary wheel compared to inching without one wheel being stationary.

4.1.3 Varied Inching Percent Tests

Seventeen more tests were run to explore the effects of varying the inching percent on the performance. This study re-used five tests from the last table at the 100% inching case. These tests would be used as a nominal inching performance to determine if varying the inching percent could outperform the perfect 100% inching. All of these tests were performed with a fast wheel speed of 2 cm/s and a slow wheel speed of 0 cm/s. At 110% and 160% only the 0% carriage slip was tested to understand if these tests fell into the same pattern. These tests are all outlined in Table 4.4.

Wheel Speed Slow:Fast(cm /s) = 0 -> 2 for all tests			Inching %					
			80%	100%	110%	120%	140%	160%
Varied Inching % and Cariage Slip %	Cariage Slip %	0%	X	X	X	X	X	X
		20%	X	X		X	X	
		40%	X	X		X	X	
		60%	X	X		X	X	
		10%	X	X		X	X	

Figure 4.4: Varied inching percent tests performed

4.1.4 Traction Control No Inching with Varied Wheel Speed Tests

Finally, the last test campaign aimed to understand if varying wheel speeds without inching could provide some benefit over the baseline tests. Ten tests were run with no inching, and the front and back wheels being run at different speeds, either 1 cm/s or 2 cm/s. These tests were run at all the different carriage slips. The carriage slip percent in this case is relative to the slower 1 cm/s wheel speed, and the other wheel will naturally have a different slip value. These tests are shown in Table 4.5.

Inching % = 0 for all tests			Wheel Speed Front:Back(cm /s)	
			1 : 2	2 : 1
Basic Two Wheels At Different Speeds and No Inching	Carriage Slip %	0%	X	X
		10%	X	X
		20%	X	X
		40%	X	X
		60%	X	X

Figure 4.5: No inching and varying wheel speed tests

4.2 Test Procedures for Consistency

To run the tests consistently the soil must be prepared the same way each time. As the wheels drive over the sand it gets compressed so the first step to prepare the new soil is to drive 10, 6 inches

tines into the soil at one end of the testbed. They are then dragged through the length of the testbed using the carriage. They are then slide over partially so that the gap between soil that was tined is cut in half and they are driven back through the soil. Pictures of the tines can be seen in Figure 4.6. Once the soil is all loosened with the tines, it needs to be flattened so the wheels can drive over it and the sinkage can be measured off the referenced flat soil. A flat bar is attached to the carriage which is then driven back and forth over the soil. This produces the final flat soil that tests can be run on.

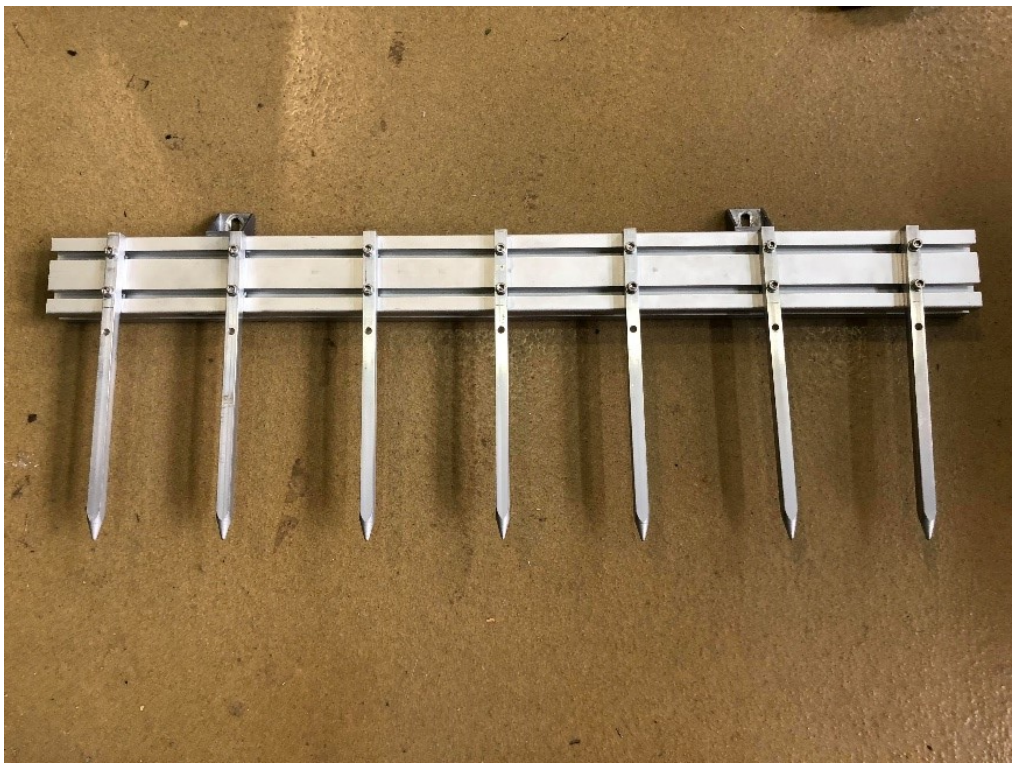

Figure 4.6: Tines used for soil preparation

The wheels are relatively narrow compared to the four feet of soil width that is prepared and flattened therefore three tests were run over different sections of the prepared soil to expedite the testing procedure. For each set of testing parameters, the tests are run in triplicate. Before each test, the bias of the force torque sensor is taken so it can be removed from all the data for that test in post processing. Wheel speeds were all run between 0 cm/s and 3 cm/s to remain consistent with nominal speeds for plausible planetary rovers of this size. Each test was run for a length of 140 cm down the prepared soil.

4.3 Summary

Five main test campaigns were completed. The first was baseline tests, where no inching was performed and the wheels drove at the same speed to characterize the nominal system performance. Secondly, perfect inching tests were completed where one wheel was always stationary as inching has been tested in the past. Perfect inching was then tested where both wheels were rotating but at different speeds, inching was still performed but one wheel was not stationary. These tests should help to prove that the static wheel is accounting for a majority of the performance increase seen with inching. The fourth test campaign was varying the inching percent away from 100% to see how that would affect performance because this is another new parameter that has never been experimented with before. Finally traction control tests were performed with the wheels driven at different speeds to determine if performance can be gained without inching. These tests were all run with the same test setup and with soil preparations performed between tests for consistency.

Chapter 5

Inching Average Drawbar Pull Coefficient Results

Results are first presented here for drawbar pull inching test results. The graphs presented show average drawbar pull coefficients versus carriage slip, inching percentage, or wheel slip. These graphs show trends for how these parameters affect the drawbar pull coefficient of the mobility system. The average values are calculated with all data collected after the first 30 cm of soil is traversed to ignore any startup abnormalities and use only steady state data. Error bars are also shown with each average value to represent the range of data seen in one test and also between the triplicate of tests run at the same conditions.

5.1 Baseline Tests

Baseline Tests were run with no inching and the wheels set in their middle distance apart. These tests were run to understand how the testbed performs under nominal conditions when not inching. These will be baseline tests to determine if the inching tests are performing better or not than traditional drive methods. Video was captured of the tests and Figure 5.1 shows various video clips from the 0% carriage slip test. A blue ruler (not made to any scale) is added in the center of each video frame for reference between frames. Notice the wheels maintain the same distance apart throughout the video. As the test rig proceeds down the testbed you can see very little sinkage into the soil and the tracks appear to have no soil shearing and simply leave little divots where the grousers dug into the soil.

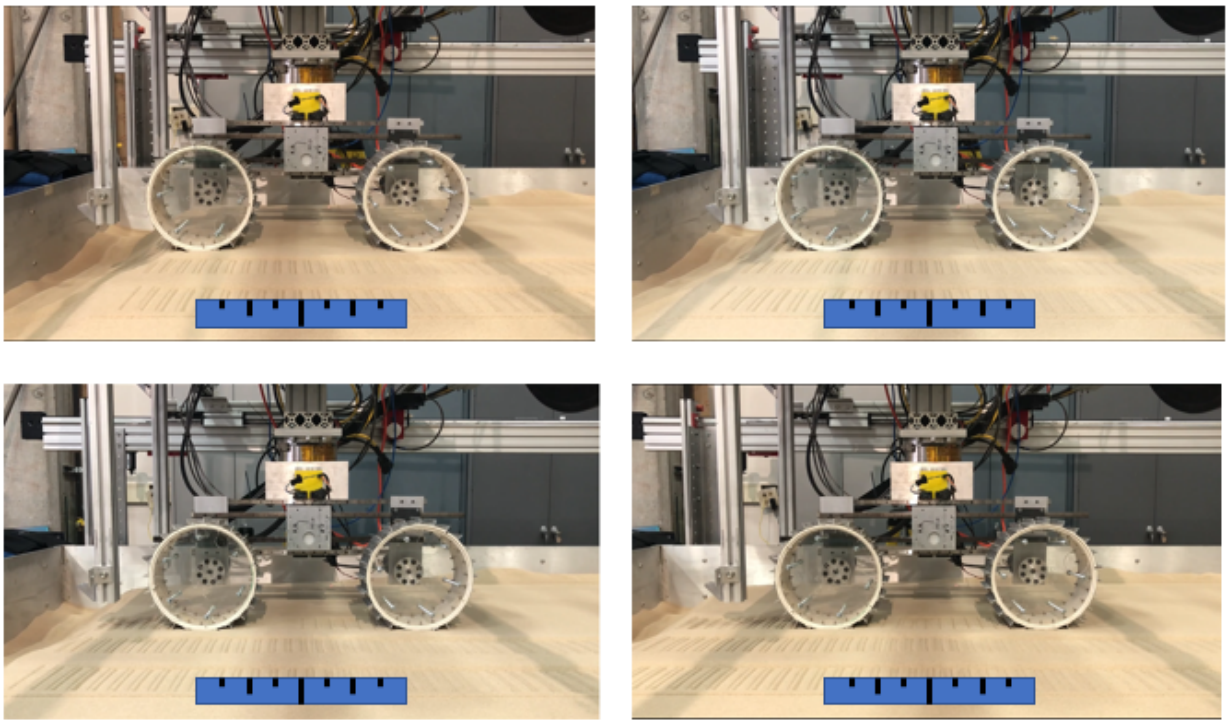

Figure 5.1: Baseline no inching test clips, 0% carriage slip, 1 cm/s wheel speeds

Baseline tests were run at two different speeds with no inching to determine if wheel speed was a contributing factor to overall performance. Tests were run with both wheels driving at 1 cm/s and at 0.5 cm/s at the 0% and 60% carriage slip values. These tests are graphed below in Figure 5.2. Since the red and black average points at the 0% and 60% slip values fall within the error bars of the opposite color, it can be concluded that these tests perform the same and therefore wheel speed does not affect performance at the low speeds tested.

The black points in Figure 5.2 were all run with both wheels at 1 cm/s at various carriage slips to characterize how carriage slip affects performance when no inching is taking place. Similarly to the work performed in Ref [17], testing single wheel performance, a similar curve is produced with the two wheels in these tests. The drawbar pull coefficient increases up through 20% slip, where the performance begins to level out while still increasing slightly through 60% slip. The highest drawbar pull coefficient achieved is around 0.145 with the value being closer to 0.14 at 20 to 40 percent slip.

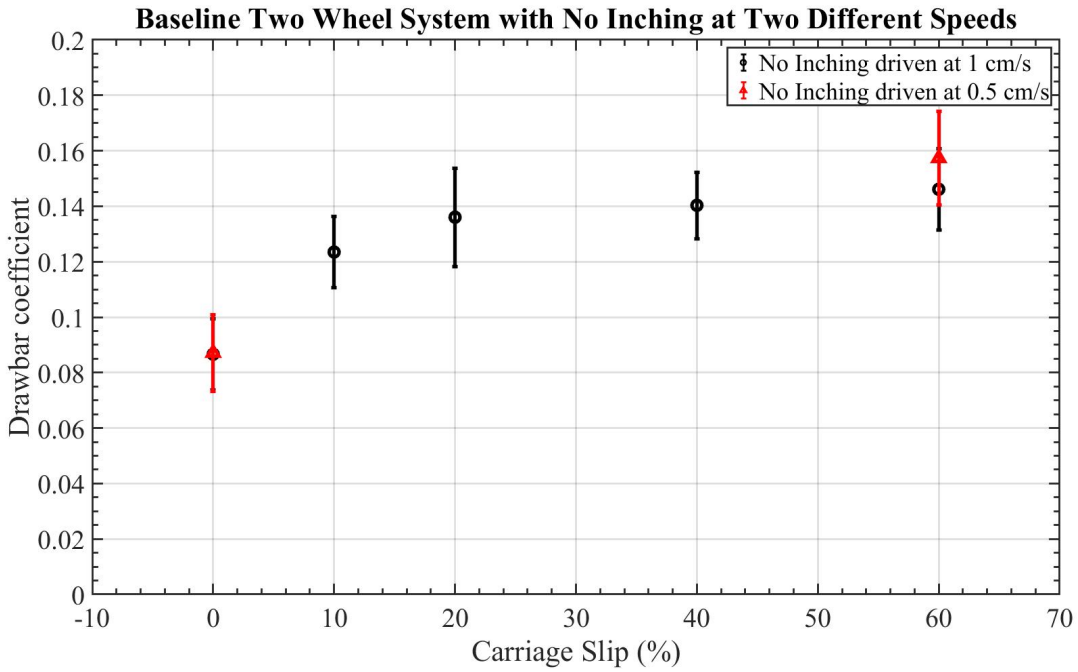

Figure 5.2: Baseline no inching test drawbar pull coefficient results

5.2 Perfect Inching Tests

These tests were all run with perfect synchronization between the expansion speed and the wheel velocities. The first set of tests were all run with one wheel not rotated. This is how inching was performed in the past with the Scarab rover and so these tests should confirm those initial results. The second set of tests were run with both wheels always moving but at different speeds while inching. These tests will help confirm that the performance increase when inching is largely due to one wheel being planted in the soil to push off of. They will also help show if some performance can be gained through this slightly faster form of inching.

5.2.1 Perfect Inching with One Stationary Wheel

A similar set of tests to the baseline tests were run for 100% inching with one stationary wheel at two different fast wheel speeds and then sweeping through all carriage slip values. These results were expected to look similar to results described in Section 1.3. Results can be seen in Figure 5.3 for these perfect inching tests. Again, the difference in wheel speeds does not change the performance so wheel speed can be taken out as a potential input parameter. Also, similarly to the non-inching case drawbar pull coefficient increases from 0%-20% and then leveling off and only increasing slightly from 20%-60% slip. The error bars in this graph are taller than the ones

in Figure 5.2. This is due to the wide variation of performance through the various inching cycles and will be described in more depth in Section 6.2.

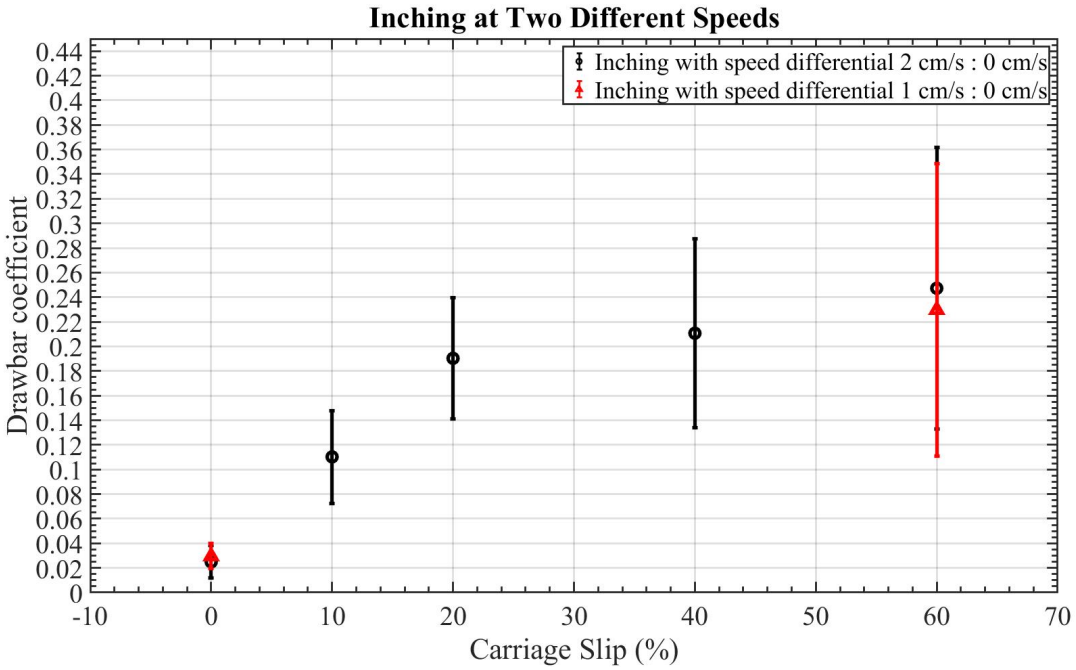

Figure 5.3: 100% inching at two different speeds

Figure 5.4 shows clips from the video of the 100% inching test run at 0% carriage slip with the wheel speeds being 2 cm/s and 0 cm/s. Frame (A) shows the wheels at almost their widest point. Then as the carriage drives forward and the wheels contract, they get to their middle point in frame (B). Notice that the rear wheel generates more tracks behind it between frame (A) and (B) but the front wheel does not generate any more tracks and is perfectly stationary relative to the sand. Frame (C) then depicts the wheels at their closest point and still the front wheel has not moved. Then frame (D) shows the middle point again with now the front wheel generating new tracks and driving forward and the rear wheel staying put in the sand. Finally, frame (E) shows the wheels expanding even more and finally reaching their maximum point once again in frame (F).

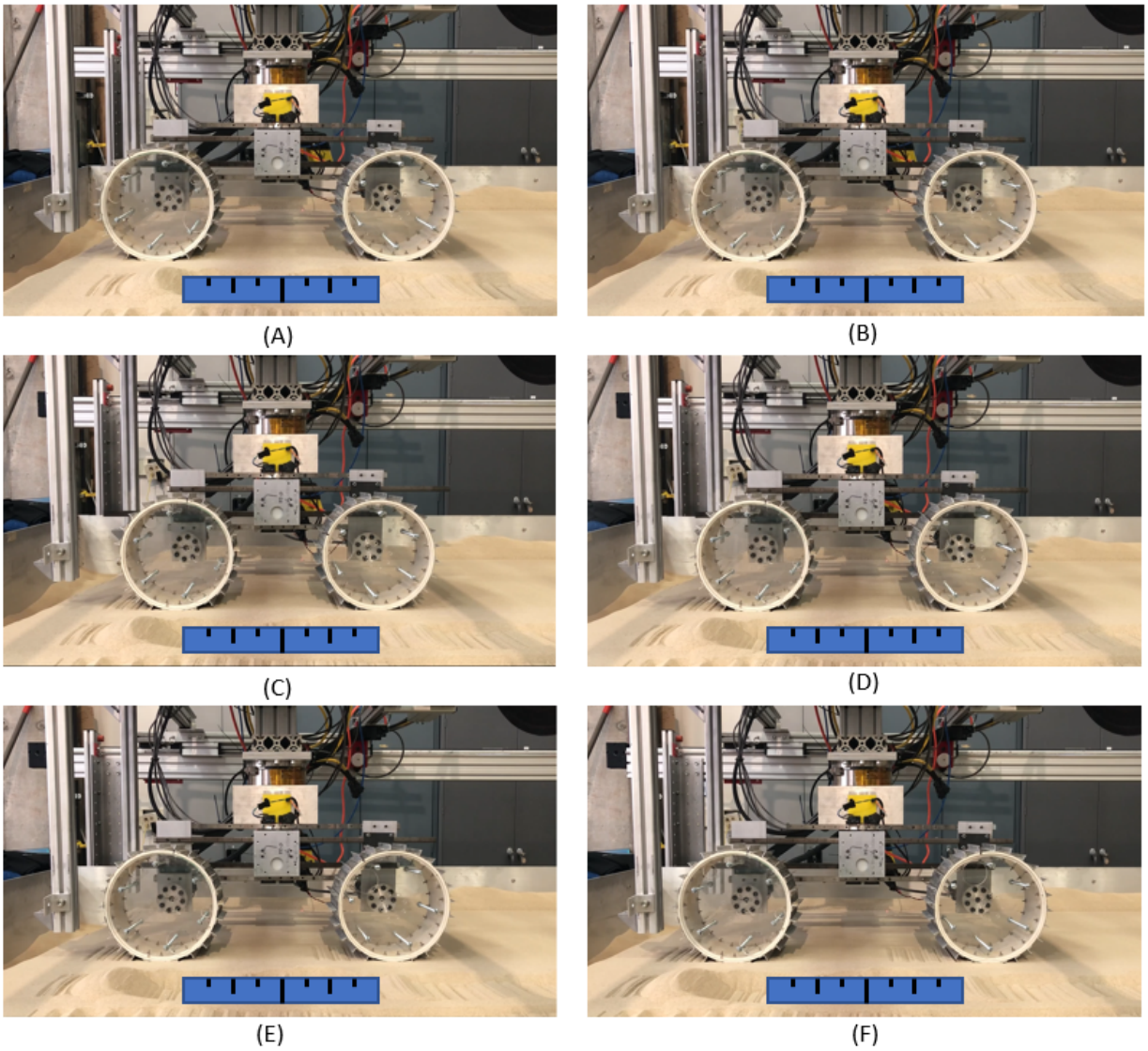

Figure 5.4: 100% inching at 0% carriage slip with wheel speeds of 0 cm/s and 2 cm/s

Figure 5.5 depicts the same 100% inching with a carriage slip of 40% instead of 0% this time. The main difference in these Images is that the tracks in the soil behind each wheel are dramatically different due to the wheel being driven faster than the carriage is moving forward so the wheels slips, the soil shears, and the soil is pushed backwards more. The rig also sinks into the soil more as this test progresses forward. These images do continue to show the distance between the wheels changing from small to medium to large compared to the added blue ruler. As the video progresses from frame (A) to (B) to (C) the wheels are expanding from their minimum distance, to the median distance, to their furthest distance apart. As this happens the front wheel drives forward generating new tracks and building a slight pile of soil behind it. The rear wheel, due to the carriage speed being slower than the expanding speed, is pushed backwards into the soil behind it. This is most

noticeable in the gap between the front edge of the rear wheel and the soil. In frame (A) there is no gap and in frame (C) there is a large gap between the front of the rear wheel and the soil. Then as the wheels contract together between frames (C) and (D) the front wheel is not turning but is being pulled backward slightly. Again, this is most noticeable where the front of the front wheel is contacting the soil. As the wheel is pulled back, it goes from pushing up against the new untouched soil, frame (C), to sitting back into the hole it has just dug, frame (D). Then between frames (D) and (E) the wheels expand again, and between (E) and (F) they contract once more.

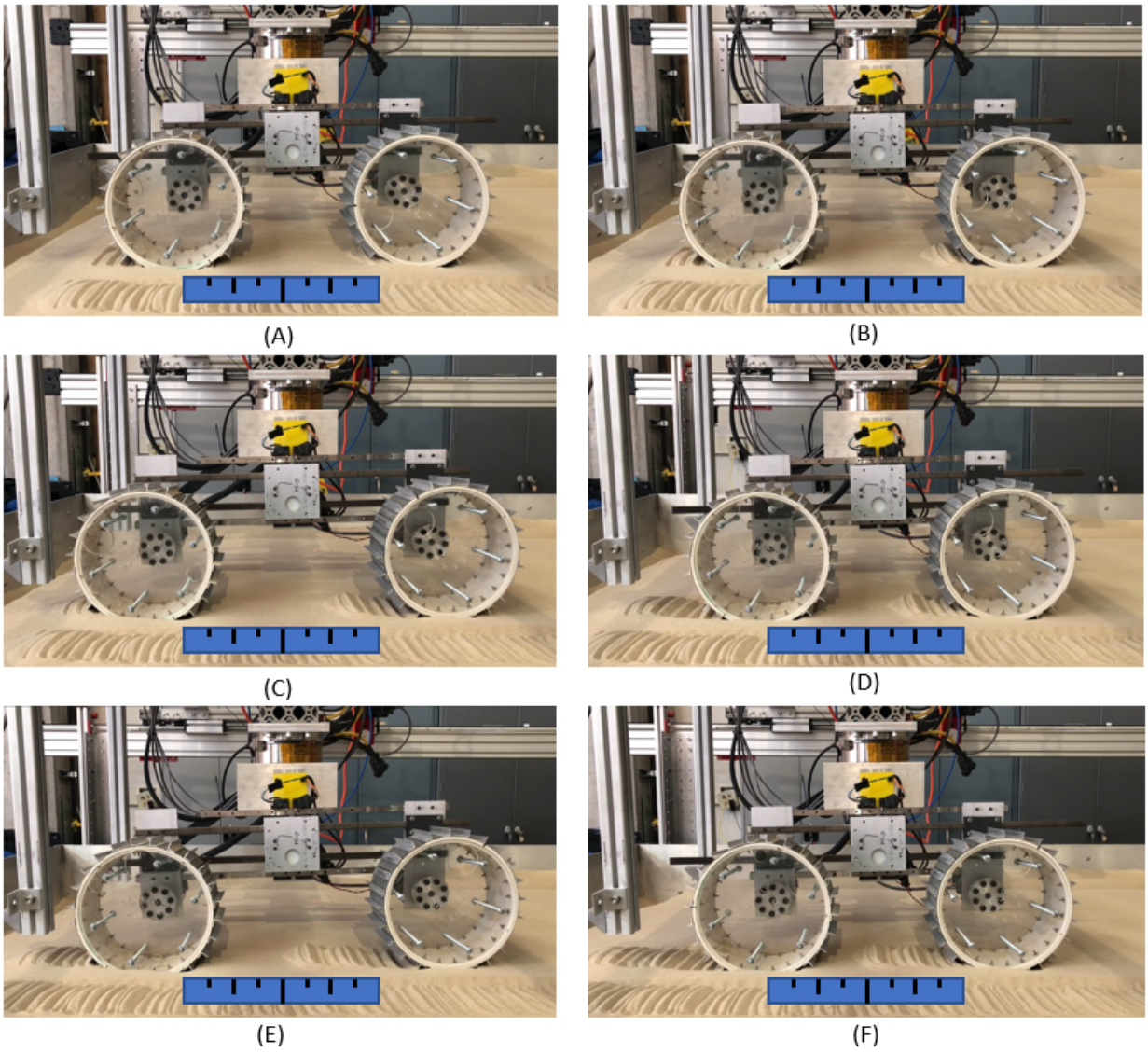

Figure 5.5: 100% inching at 40% carriage slip with wheel speeds of 0 cm/s and 2 cm/s

Figure 5.6 compares the full sweep of inching tests to the full sweep of baseline tests. Note the two tests that lie on non-perfect slip values were ran self-propelled without controlled slip.

To accomplish this the carriage motor was disengaged and the wheels themselves propelled the carriage forward. The reported slip values for those tests were measured once the test reached a steady state slip value. It is shown here that at 0% slip the baseline test outperforms the inching test. This result was unexpected and therefore is explored more thoroughly in Section 6.1. However, once the tests reach 20% slip the inching test is outperforming the baseline as expected. The difference between the baseline and inching test becomes larger as the slip increases past 20%. Due to the wheel speeds used in these tests the carriage speeds are identical between the tests at each different carriage slip value. This means that better performance can be achieved through inching while the same overall robot speed, in this case carriage speed, can be maintained.

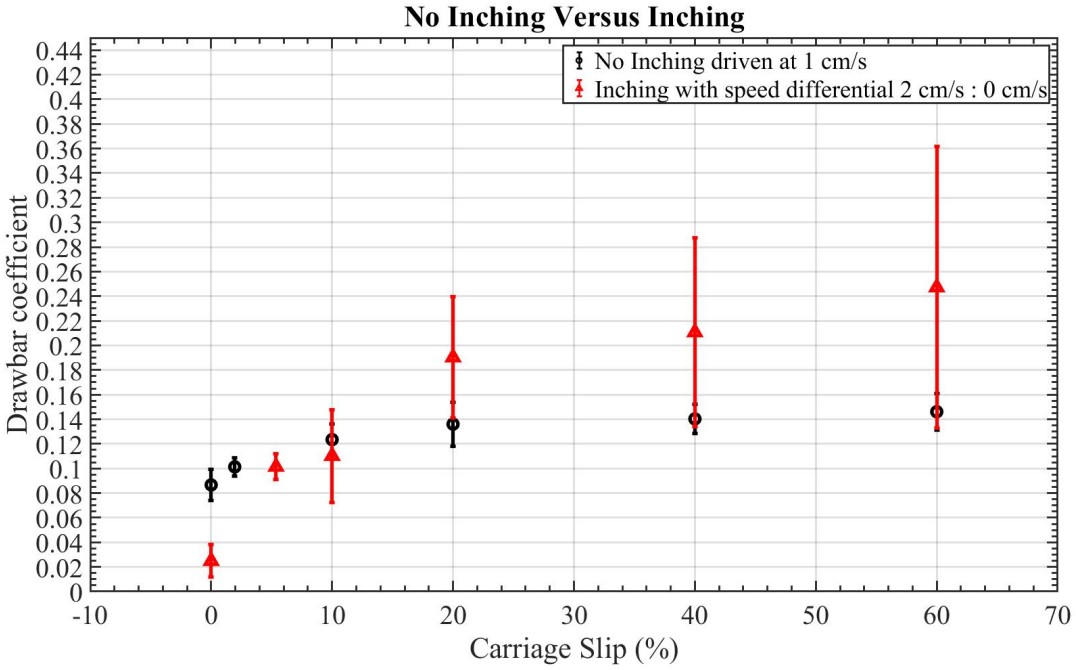

Figure 5.6: Baseline versus inching drawbar pull coefficient results

5.2.2 Perfect Inching With Two Moving Wheels

Traditional inching, as it has been studied in the past has always been with one wheel completely static and not moving. The next set of tests were run with both wheels moving while the inching was performed. This type of inching would be faster than leaving one wheel stationary and these tests were run to determine if some of the benefits from inching could still be achieved through this type of inching. Frames taken from a video of one of these such tests where the fast wheel speed was 3 cm/s and the slow wheel speed was 1 cm/s. The test was run at 100% inching and 0% carriage slip and is shown in Figure 5.7. Between frames (A), (B), and (C) notice the distance between the wheels going from maximum to minimum. However, unlike previous video clips both wheels continue to move forward in the sand and leave tracks behind them with the rear wheel

adding more tracks behind it than the front wheel does. Then between frames (C) and (D) the wheels fully expand and so forth. Notice that again there is no soil build up appearing because there is no wheel slip.

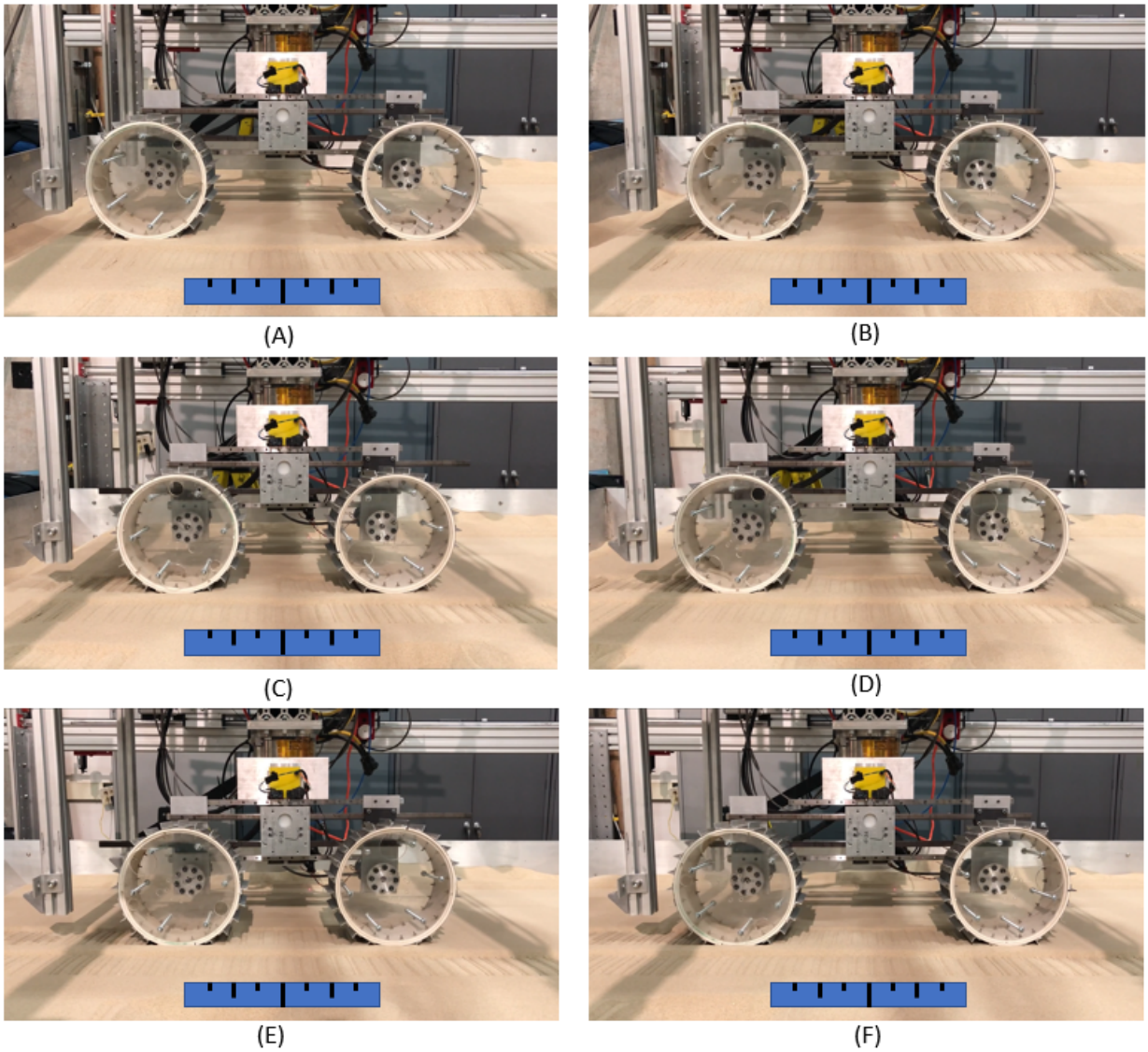

Figure 5.7: 100% inching at 0% carriage slip with wheel speeds of 1 cm/s and 3 cm/s

The results shown in Figure 5.8, show the performance of the baseline tests versus the traditional inching versus inching where the slower wheel speed is not zero but is 1 cm/s instead. The faster wheel speed for these tests is then increased from 2 cm/s to 3 cm/s to keep the difference between the speeds the same. From 20% carriage slip and up the best performance is from the traditional inching, while the inching with both wheels still turning still outperforms the baseline tests. However, at the lower slip values of 0% and 10% carriage slip the inching with both wheels still turning

outperforms the traditional inching. This is explained further in Section 6.1. The inching test with both wheels turning has a similar curve on its own, but it has more of a constant drawbar pull coefficient starting at 10% instead of 20% inching.

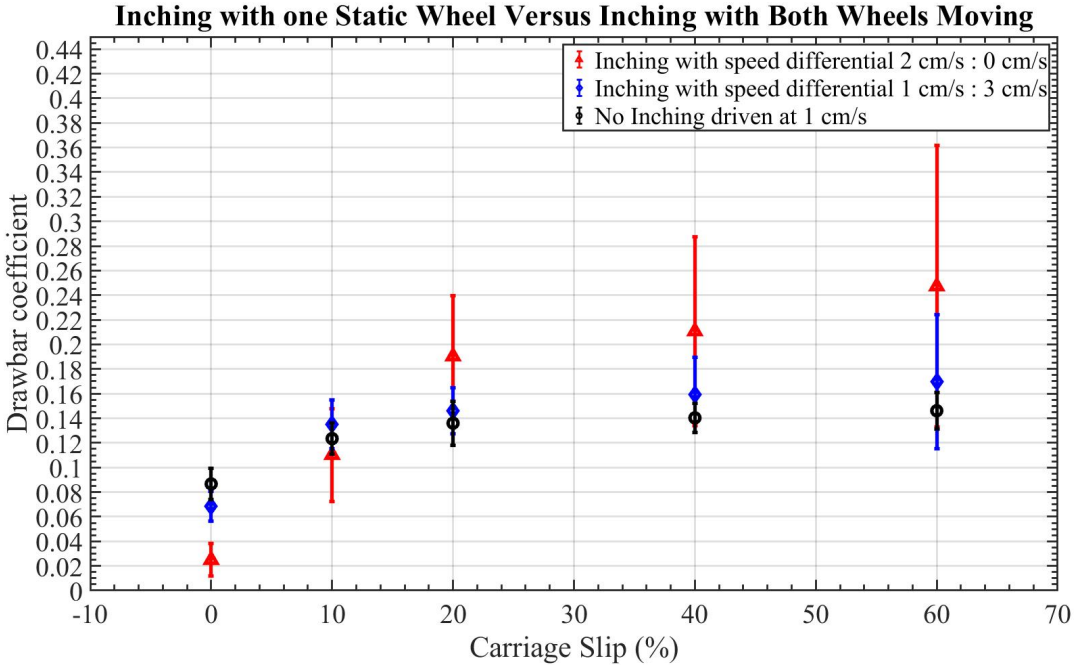

Figure 5.8: Traditional inching versus inching with two static wheels

5.3 Varied Inching Percent Tests

Inching percent is the next variable that was tested. These tests were run because the expansion speed is a degree of freedom that can be controlled and has not been tested yet with regards to inching. Inching or decreasing this was predicted to increase or decrease performance. Figure 5.9 and Figure 5.5 show two tests both run at 40% carriage slip but Figure 5.5 is video clips of the 100% inching and Figure 5.9 is 120% Inching. The difference between these two tests is how fast the expansion is driven, this causes the static wheel to be pushed forward and backwards much faster in Figure 5.9. Frame (D) shows the wheels at their closest state, so the back wheel just finished driving forward. Behind that rear wheel there are two types of tracks, the tracks directly behind the wheel are flat and show very little shearing, however, the tracks further from the wheel show shearing and are pilled up higher than the flattened soil. Then in frame (E) after only the front wheel was driven forward there are significantly fewer tracks behind the back wheel and they are all pushed up above the flattened soil. This is because the back wheel was pushed backwards by the faster expansion rate. A similar pattern can be seen behind the front wheel between frames (E) and (F). Due to the faster expansion rate, the driven wheel is actually slipping less in Figure 5.9

than in is in Figure 5.5. This manifests itself in the difference between the tracks behind the front wheel in Figure 5.9, frame (C) and the tracks behind the front wheel in Figure 5.5, frame (C). The tracks in Figure 5.9 have sheared less initially until they are modified by the wheel being pushed backwards in the following inching cycle.

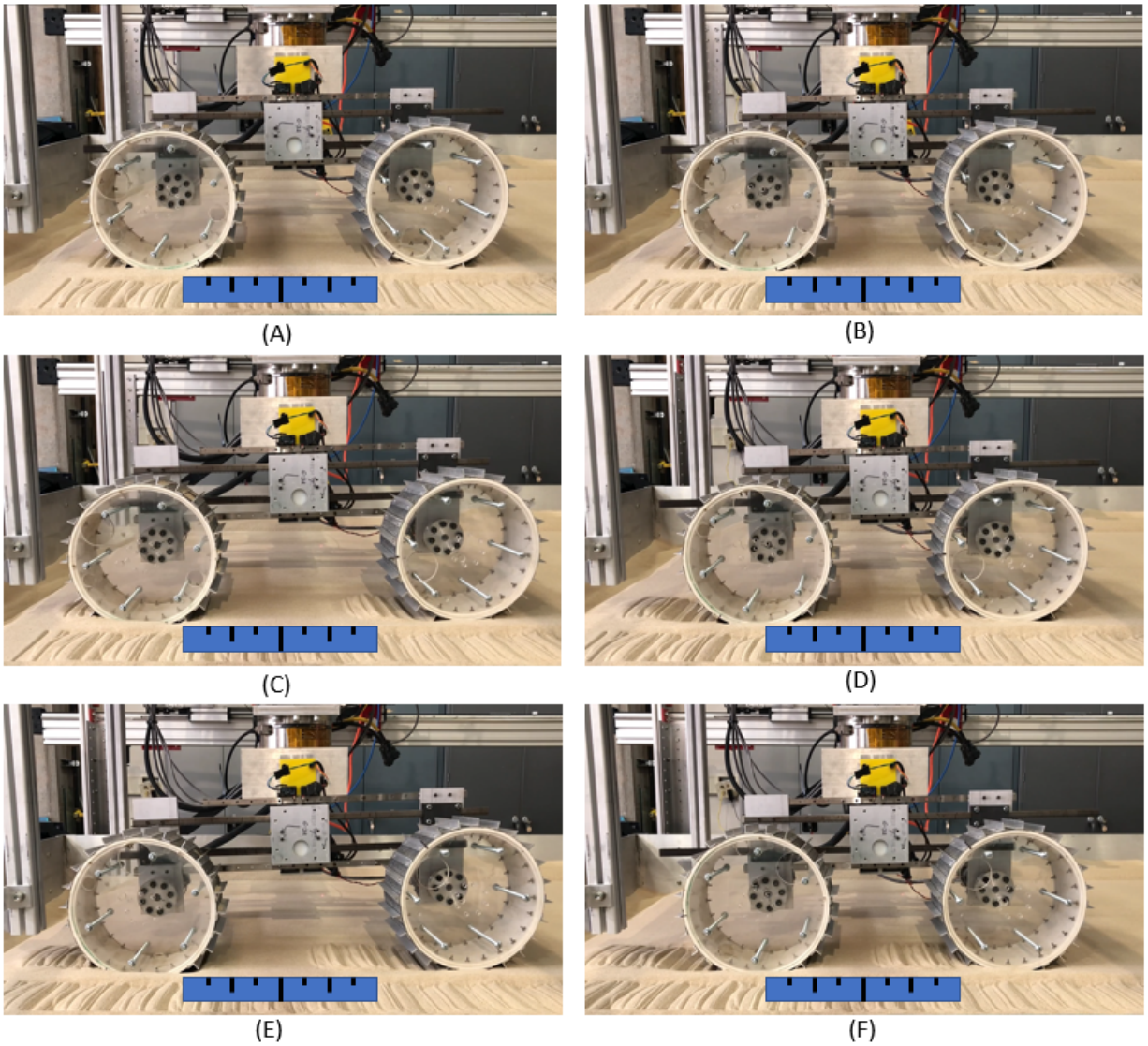

Figure 5.9: 120% inching at 40% carriage slip with wheel speeds of 0 cm/s and 2 cm/s

The results shown in Figure 5.10 start to investigate how the inching percent affects the drawbar pull coefficient. All these tests were run with inching where one wheel is not driven. Looking at Figure 5.10, no great trends were discovered. At lower slips 120% inching outperformed all the others, including the 140% inching which was unexpected. Usually as carriage slip increases so does performance so it was expected that inching percent would have a similar effect, however

this was not the case. At higher slip values, 80% and 100% inching have similar drawbar pull coefficients that are the highest, but it is unclear as to why those two perform the same when the 120% and 140% inching cases do not.

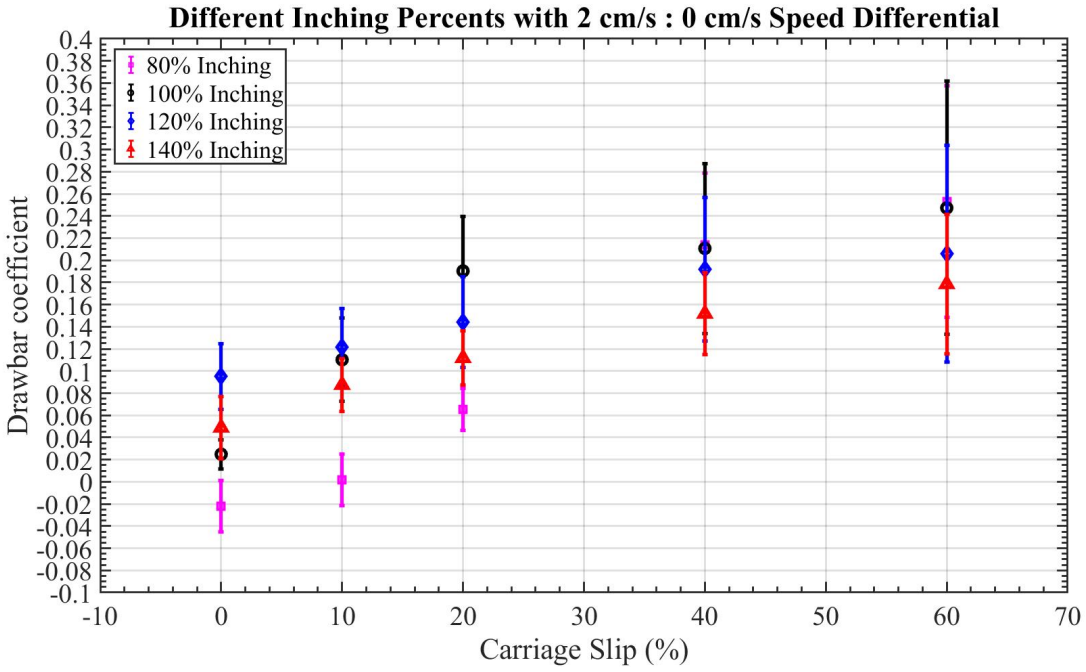

Figure 5.10: Varied inching percents with wheel speeds of 0 cm/s and 2 cm/s

Since performance is directly related to how the wheels interact with the soil and not by inching percent or carriage slip, new parameters are defined to represent these wheel soil interactions. The first parameter is the wheel slip of the faster, driven wheel. Unlike carriage slip, the fast wheel slip is the actual slip of the wheel relative to the soil and is not the slip of the whole vehicle overall.

The fast wheel slip during inching can be calculated using the combined speeds of the carriage velocity and the expansion velocity. Since these two linear velocities combined equal the total horizontal speed of the wheel. The fast wheel slip was then calculated using Equation 5.1. For reference the velocities used in the calculation are described in Figure 5.11.

Since for all these tests the slow wheel had an angular velocity of 0, which would end up in the denominator, the wheel slip of the slow wheel can not be calculated. However the horizontal speed the slow wheel is being dragged at can be calculated, Equation 5.2. This horizontal speed is the carriage forward velocity minus the expansion reverse velocity. If this number is positive the wheel is dragged forward through the testbed and if it is negative it is dragged backwards through the testbed.

$$fst_{\%} = (1 - \frac{V_{car} - V_{exp}}{V_{fst}}) * 100 \tag{5.1}$$

$$V_{slw} = V_{car} - V_{exp} \tag{5.2}$$

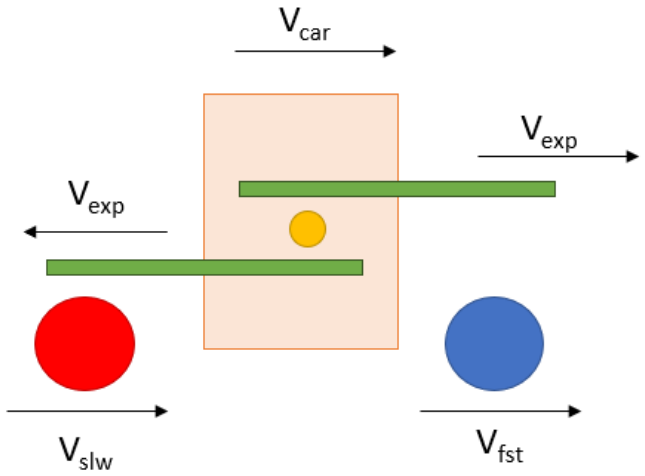

Figure 5.11: Two-wheel mechanism velocities

Figure 5.12 now plots the various inching percent data relative to the actual fast wheel slip instead of the commanded inching percent. Written in black next to each data point is the horizontal speed of the slow wheel calculated for each test. In this plot there appears to be a maximum curve where many tests correlate. Then there are five tests that fall dramatically below the curve. All tests that fall on the maximum curve have a horizontal speed that less than or equal to -0.2, whereas the points that dont fall on the curve have horizontal speeds greater than -0.2. This shows that tests with equivalent wheel slip perform the same, whether that wheel slip is caused by carriage slip of by inching percent as long as the stationary wheel is being pushed backwards by at least 0.2 cm/s. The maximum curve looks like the other curves that have been observed where it starts to level out some and not increase as steeply around 20% wheel slip.

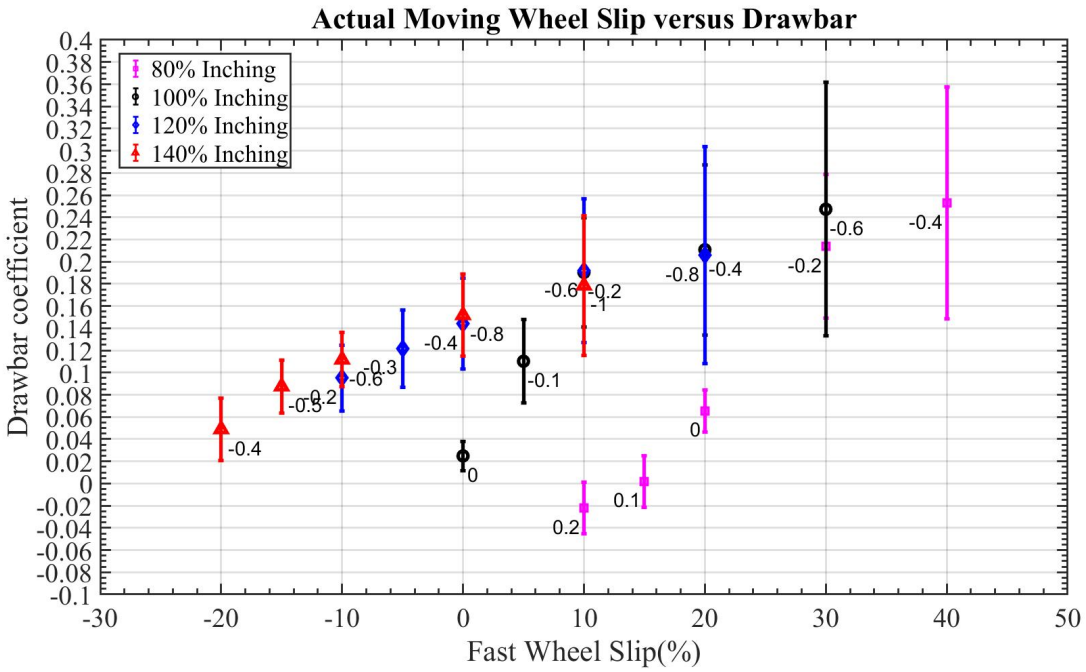

Figure 5.12: Varied inching percents with wheel speeds of 0 cm/s and 2 cm/s

5.4 Summary

First, wheel speed was shown to not affect performance of either baseline or inching tests. Both inching and baseline tests showed a drawbar pull curve similar to single wheel tests with performance increasing linearly from 0% to 20% carriage slip and then leveling out from 20% to 60% carriage slip. This shows that even when inching wheel soil interactions still drive overall performance.

At low slip values, below 20% baseline tests outperformed inching tests. This was an unexpected result and so further tests were conducted to investigate this behavior, these further test results are discussed in Section 6.1.

Inching tests were shown to considerable outperform baseline tests at slip values above 20% and continued to outperform by larger margins the higher the slip is. This is what was expected based on previous results and does hold true when tests were performed at a wide range of constant slips.

Performance was shown to be highly correlated to actual wheel slip and not carriage slip when inching percent was varied. No differences were observed if that wheel slip was caused by carriage slip or by inching percent. Tests are identical relative to wheel slip as long as the stationary wheel is pushed backwards at a rate of 0.2 cm/s or more. Sliding the wheel backwards can be produced either through carriage slip or through a slower inching percent. This means if the overall slip of

a robot is known, the necessary performance could be achieved through increasing or decreasing inching percent until the desired wheel slip is achieved. Inching therefore adds one more degree of control that will allow performance to be increased without increasing vehicle slip.

Chapter 6

Miscellaneous Study Results

The following results come from miscellaneous studies beyond the original study of inching drive versus conventional drive. Many of these studies were performed to get a better sense for specific discrepancies in the original tests, or to attempt to get a more in depth understanding of why some of the tests performed they way they did.

The first discrepancy analyzed is the results that showed at lower slip values the baseline tests outperform the inching tests, which was not an expected result. The second discrepancy is the large variation in inching performance in just a single test. The inching cycles are analyzed in more depth as they progress through time. Finally, a brief study was conducted without inching to understand if traction control in sand could be useful.

Many of these graphs analyze test results versus time. These graphs are presented to analyze further how individual tests progress and the various characteristics present over time. These graphs are created from just one test, and not the triplicate of tests are represent raw data collected from the testbed.

6.1 Low Slip Performance Discrepancy

It was shown in Section 5.2.1 that at low slips (0% to 10% carriage slip) the baseline non-inching drive out performed or performed similarly to the inching mechanism. To explore why this might be the case, inching and baseline tests were performed with a self-propelled carriage that was only driven forward by the wheels pulling against the sand and not by a driven carriage. When these tests were run it was clear that the carriage velocity was varying considerably more with the inching drive than it was with the normal drive. This carriage velocity over time for these two tests is shown in Figure 6.1.

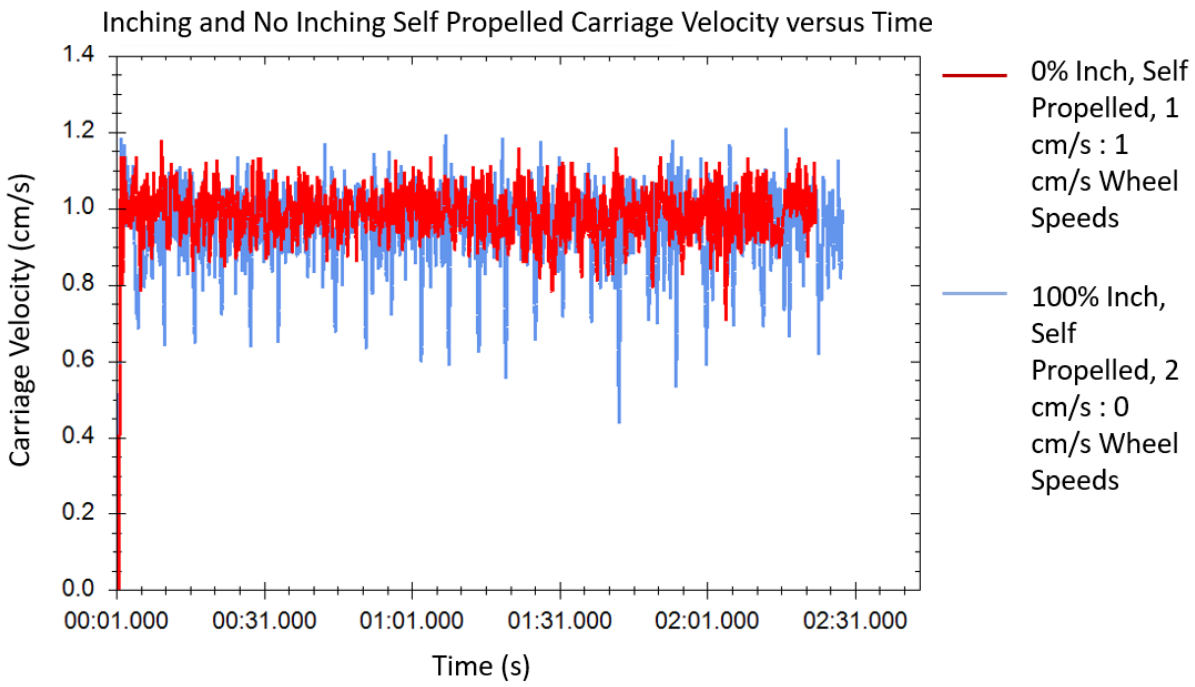

Figure 6.1: Measured carriage velocity over time of self propelled tests

This varying velocity is caused by the simplistic inching controller. The change from expanding to contracting is controlled entirely with two limit switches. When a limit switch is hit, all motors are briefly set to a velocity of zero and then quickly re-set to the proper new velocities. In a self-propelled test, as is shown in Figure 6.1 with the blue plot, this causes the carriage velocity to dip significantly at the end of each inching cycle. The average carriage velocity of the inching mechanism when self-propelled was 0.94 cm/s when the non-inching drive produced an average velocity of 0.98 cm/s. This disparity comes from the starting and stopping of the inching where the carriage velocity drops after each cycle and then takes some time to build back up to full speed.

At low slips of 0% and 10% the carriage is driven at 1 cm/s or 0.9 cm/s. In the self-propelled case the carriage velocity commonly dropped below 0.8 cm/s meaning that at low slip values the driven carriage would push the test rig forward at the end of each cycle instead of the rig pulling against the carriage. The carriage pushing will create significantly lower drawbar pull coefficient, and drop the overall average inching performance.

At the 0% carriage slip value, it takes the baseline test over 20 seconds of running to build up to its maximum horizontal force as is shown in Figure 6.2. Each inching cycle, shown in the blue plot in Figure 6.2, only runs for about 10 seconds before it reaches the end of its cycle. At the end of the cycle the velocity generated by the inching momentarily drops low and the generated force therefore drops too. Because of the short length of the inching cycle, the inching test can never build up to its full drawbar pull potential and results in an average drawbar pull that is considerably lower than the non-inching case.

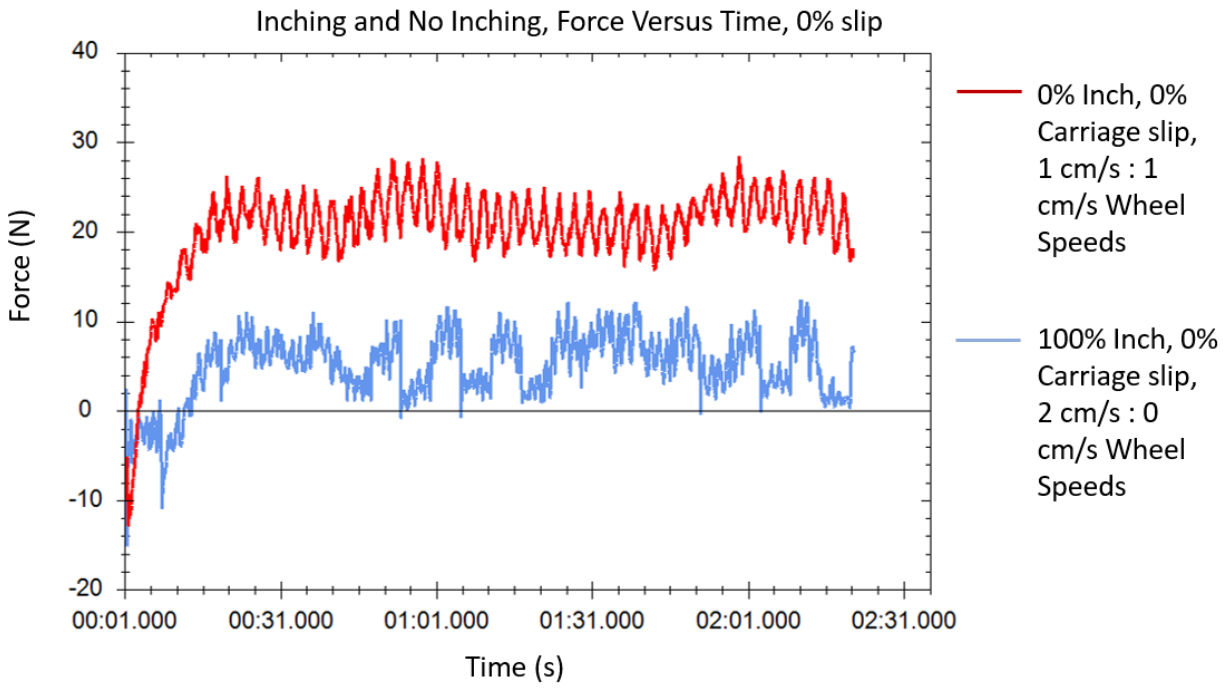

Figure 6.2: Measured horizontal force over time of inching and baseline tests at 0% slip

This fact is further proven by comparing the forces generated over time by the self-propelled tests in Figure 6.3. These tests were run without driving the carriage, and both tests inching and baseline perform the same. When the velocity of the carriage is not a factor, the inching and baseline tests produce the same force. Therefore if the carriage speed and two-wheel mechanism speeds were perfectly synchronized to cause 0% slip constantly the baseline tests and inching tests should perform the same as they do in these self propelled tests.

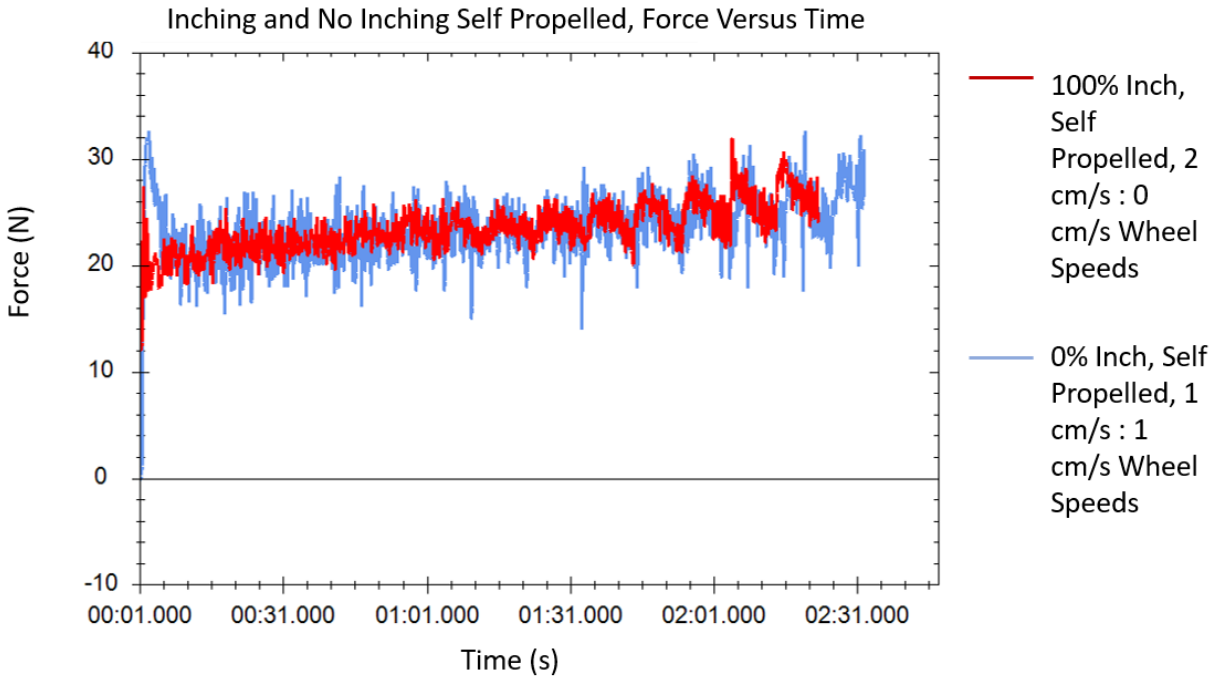

Figure 6.3: Measured horizontal force over time of inching and baseline self propelled tests

For all these reasons, the baseline tests outperforming the inching tests at low slips is due to the inching controller and inching testbed. The stopping and starting affects the natural carriage velocity causing the driven carriage to artificially lower results. The short length of the inching mechanism means the inching doesn't have enough time to build up to the same drawbar pull coefficient as its baseline counterpart at low slips.

When the inching case where both wheels are driven is analyzed with respect to time, there are similar cyclic trends that occur with traditional inching. This plot is shown in Figure 6.4. In this case the wheels never stop moving but just switch between 1 cm/s and 2 cm/s. Due to this behavior the carriage velocity generated by the inching does not drop nearly as much. Towards the end of each cycle the Force reaches close to the 20 N mark where the baseline test for 0% slip was performing. Due to the stopping and restarting at the end of each cycle the force still drops giving this test a worse average performance than the baseline test but a better performance than the traditional inching as the velocity does not drop as much.

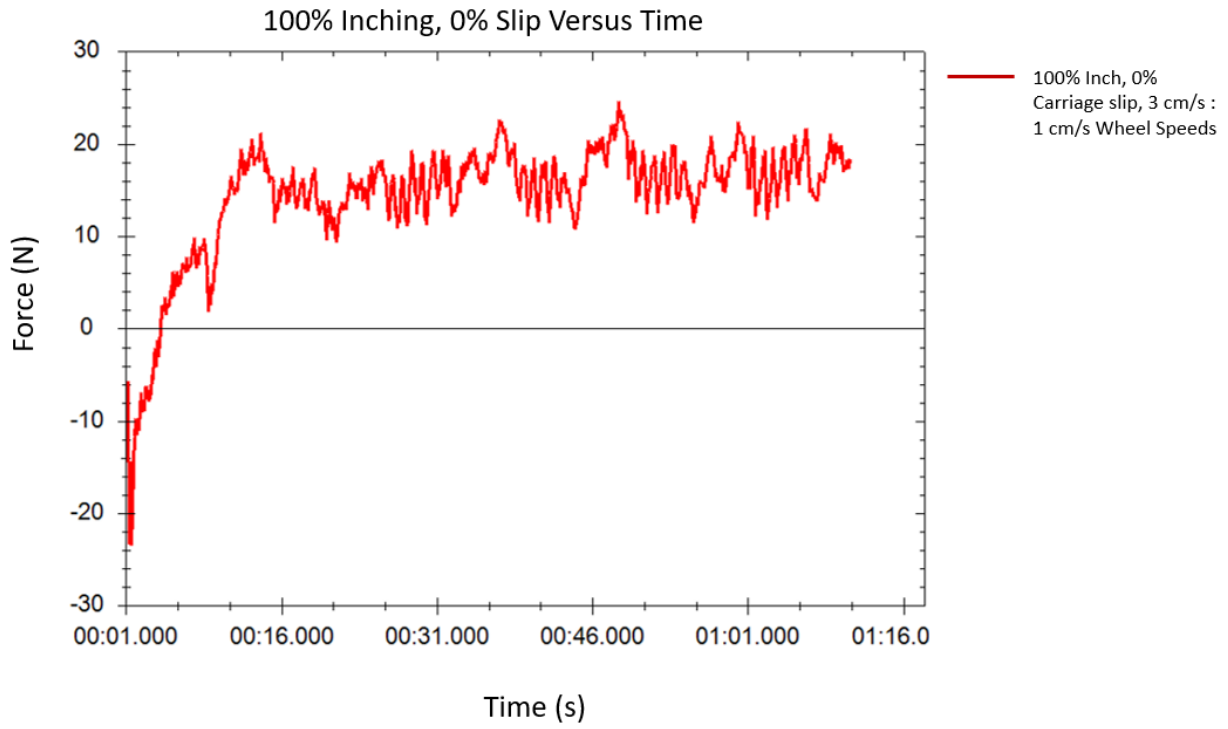

Figure 6.4: Measured horizontal force over time of inching with no slip and 1 cm/s to 3 cm/s wheel speed differential

6.2 Large Error Bars for Inching Tests

Another major difference between the baseline and inching tests was the size of the error bars for the drawbar pull results. It was hypothesized that these large error bars come naturally from the inching cycles, as the mechanism switches in between expanding and contracting. To investigate this discrepancy further some inching and non-inching individual tests were compared over time instead of as average values.

At high slip values, for example 60% carriage slip as is shown in Figure 6.5, the dramatic cyclic behavior of the inching tests is clearly present. As the inching cycle changes, the horizontal force still drops to where the baseline test is. However, at high slip values the inching out performs the baseline by so much that the force quickly rises back up dramatically above the baseline test. Due to this behavior the average value of the inching tests is dramatically higher than the baseline tests, although even at these high slip values in Figure 5.6 the error bars of the inching test still drop to the same drawbar pull coefficient as the baseline tests.

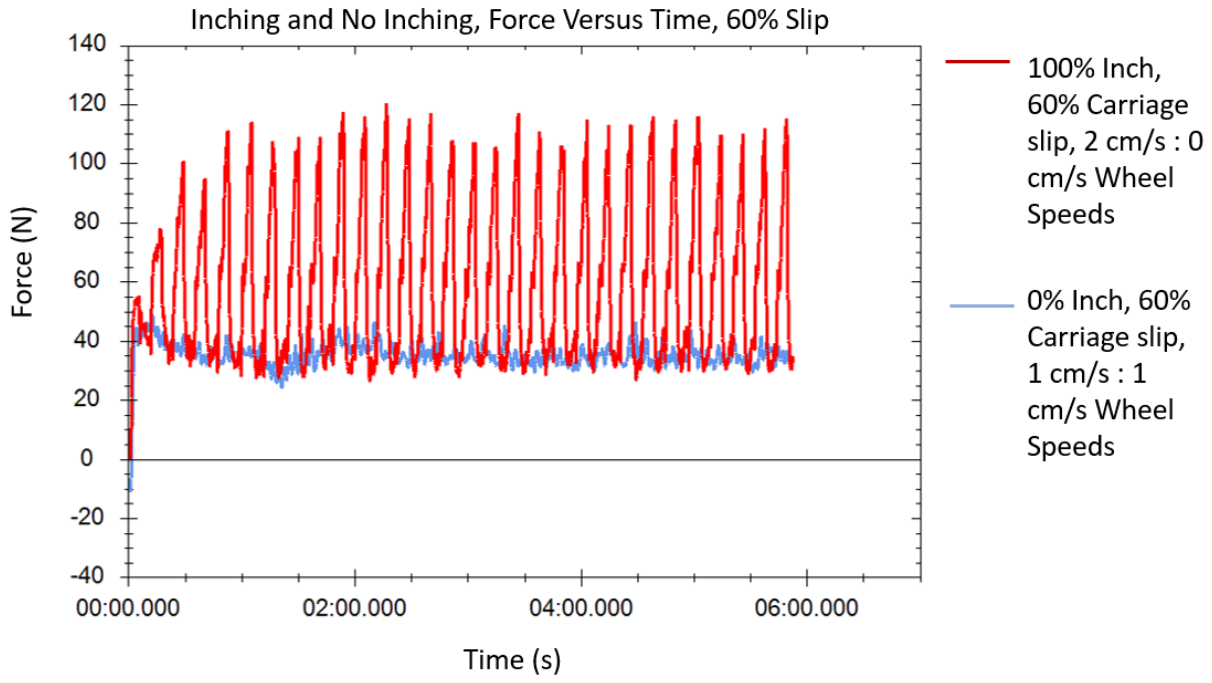

Figure 6.5: Measured horizontal force over time of inching and baseline tests at 60% slip

6.3 Inching Cyclic Performance

There is large variations in performance throughout the inching cycle as was observed in Section 6.2. This cyclic behavior was therefore investigated further to attempt to understand what is causing this dramatic difference in performance. This understanding might help to improve performance overall in the future if the lower performing areas of the cycles can be raised up with the higher performing times in the cycle.

Figure 6.6 shows a 100% inching test run at 20% carriage slip over time versus horizontal force. The test was segmented by every large drop in force. A video of the test was then used to count how many cycles were completed and which cycles in the graph were expanding versus contracting. The expanding sections are marked with a white background and the contracting sections are marked with a grey background. This test distinctly shows that the expanding sections produce significantly higher forces than the contracting segments do.

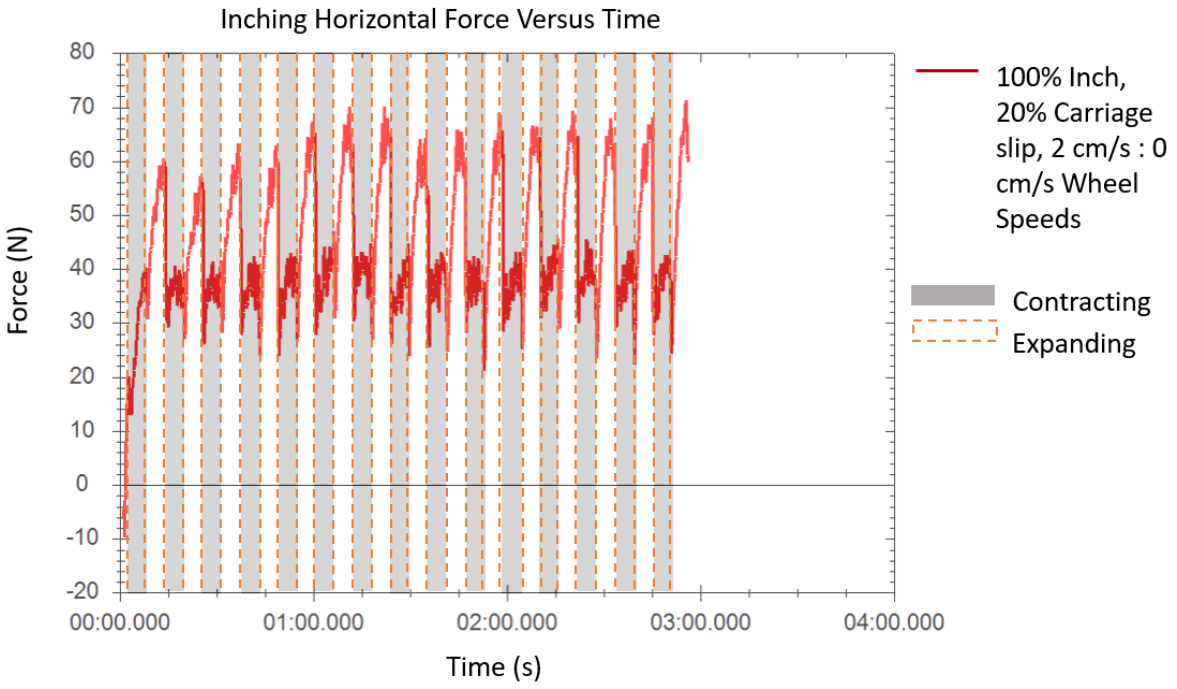

Figure 6.6: Measured horizontal force over time of inching with 20% slip and sectioned by inching cycle

This pattern is also visible, but less obvious, at the 0% slip amount and is shown in Figure 6.7. At high slip rates the difference is more dramatic. The high spikes visible in Figure 6.5 are from expanding while the contracting force values stay lower near the baseline force values. Unlike the lower slip graphs the 60% slip expanding cycle never reaches steady state and appears to create a high spike before it drops back down again.

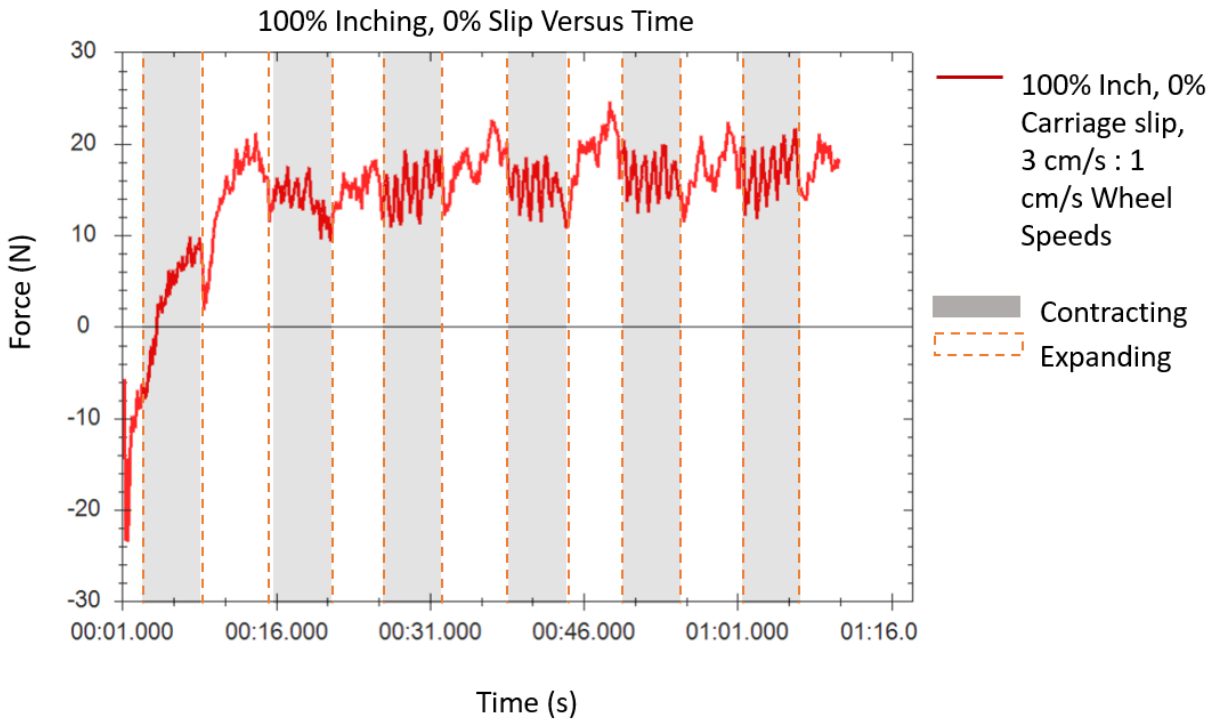

Figure 6.7: Measured horizontal force over time of inching with no slip and sectioned by inching cycle

6.4 No Inching with Traction Control Results

Tests were run finally with no inching but with the wheels moving at different speeds. These tests were completed to explore how traction control in sand could be beneficial. It was hypothesized that some of the benefits of inching come from digging one wheel into the soil more than another and maybe this behavior could be replicated by driving one wheel faster than another.

Video clips from the tests that were run with no inching, but with varying wheel speeds are shown in Figure 6.8. The test shown was run with the back wheel driven at 2 cm/s and the front wheel driven at 1 cm/s. The test was also performed at 20% carriage slip relative to the slower 1 cm/s wheel speed. As the test progresses through the frames the back wheel sinks more into the soil giving the whole mechanism an angle and the wheels remain the same distance apart.

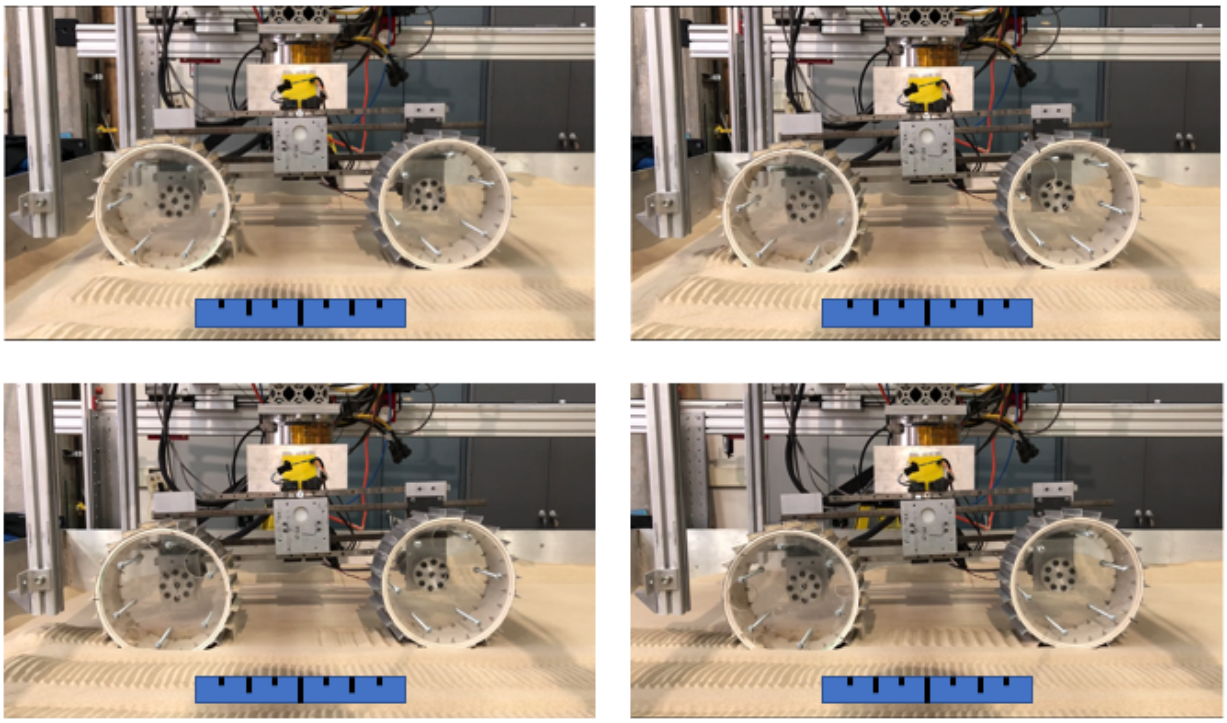

Figure 6.8: No inching and 20% slip with the front wheel velocity of 1 cm/s and a rear wheel velocity of 2 cm/s

Test results for all such non-inching with differential wheel speeds are shown below in Figure 6.9. Throughout all the carriage slip values, the test with the back wheel speed twice as fast as the front wheel speed outperformed the other tests.

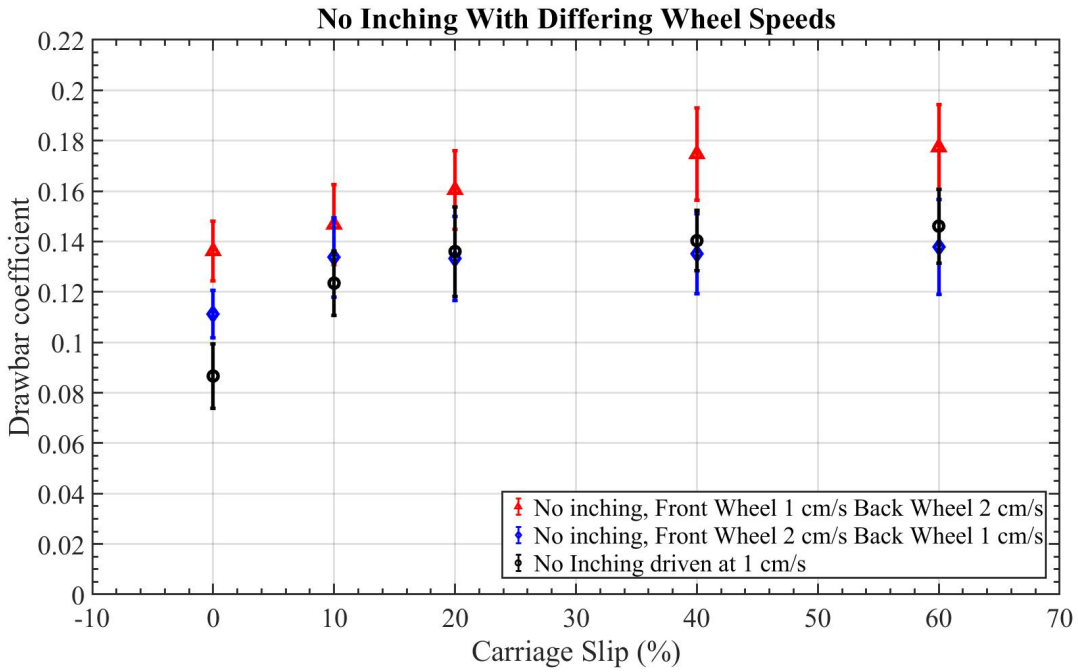

Figure 6.9: No inching and differing front and rear wheel speeds

Combining these results with the results discussed in Section 6.3 about inching cycle differences, provide insights into why this behavior is happening. Both these results show when the back wheel is being pushed off of the tests get higher results then when pulled by the front wheel. This pattern is seen when expanding during inching and when driving the back wheel faster and not inching. This is due in part to the mechanism leaning backwards in both these cases, helping the front wheel get over the sand and the back pushing wheel is digging into the deeper, more compact soil to get even more traction. Secondly this is the case because when the front wheel is driven faster or the inching mechanism in contracting, the rear wheel is driving over a high pile of soil generated by the front wheel. This produces more of an obstacle in these cases than is present when the back wheel builds up a soil pile and the mechanism does not have to traverse it.

6.5 Summary

It is hypothesized, based on these studies and the operation of the testbed that the results at low slip values are not accurate. Test results show that baseline performance is above inching performance, but this analysis suggests these results are coming from unsynchronization between the two-wheel mechanism controller and the carriage controller.

Large error bars for all the inching tests, compared to the error bars present for baseline tests, are resulting from a large cyclic variation in drawbar pull results from the inching mechanism. When

the inching mechanism reaches the end of one of it's cycles, the performance drops back close to the baseline performance but the quickly raises back up as the cycle continues on.

This large inching cycle discrepancy is then shown to not occur with each cycle but to only spike higher with every expanding cycle. The expanding cycles are all performing considerably better than the contracting cycles. This result is related to the traction control study where driving the rear wheel faster than the front wheel and not inching is better than driving the front wheel faster. This result is hypothesized to be resulting from the different angle of the testbed, either angled up helping to drive over the sand or angled down and bulldozing more of the sand in front of it as it drives forward. It is also resulting from the pile of sand from the faster wheel either being built up between the wheels, hindering forward progress, or being built up behind the robot entirely not hindering progress.

Chapter 7

Inching Average Sinkage Results

Besides drawbar pull coefficient, the other metric that is considered important for planetary exploration mobility systems is their sinkage into loose soil. Figure 7.1 shows the steady state sinkage value of the tests comparing baseline tests to inching tests. While there are some small differences between some of the tests for the most part the averages are within the error bars of the other tests and there is no significant difference. At 0% and 10% slip the no inching sinkage is below the inching error bars, however the difference between the average sinkage is around 3 mm which is just 2% of the wheel radius which is very small.

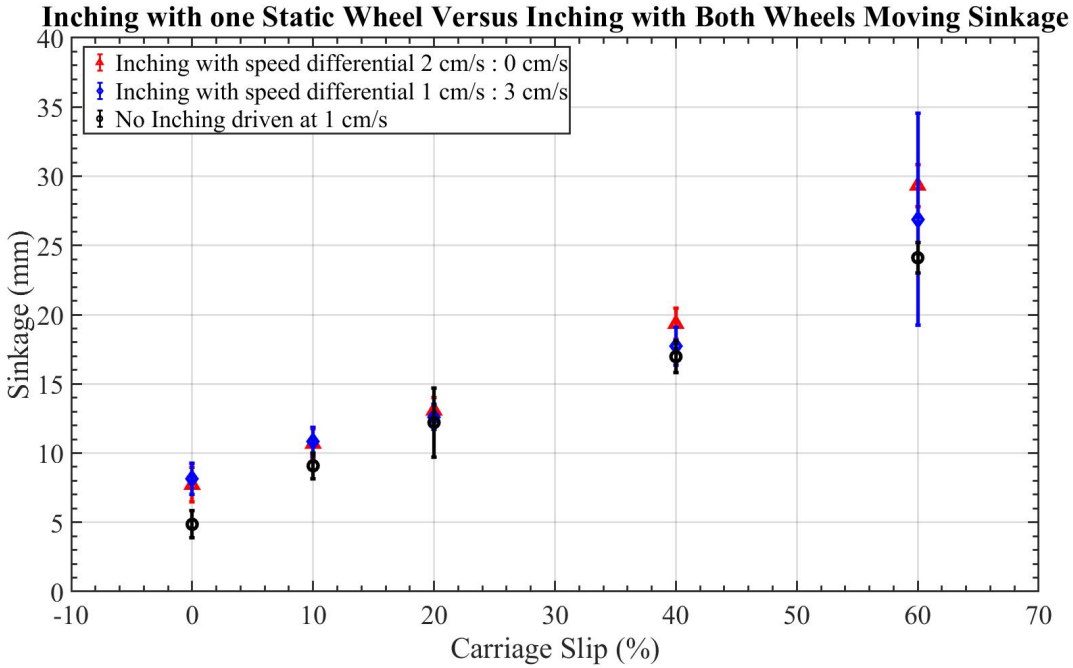

Figure 7.1: Sinkage values of inching compared to baseline tests

Figure 7.2 compares the sinkage for the different inching percentages and again there is a small difference in some of the tests but not more than 5 mm which is relatively small.

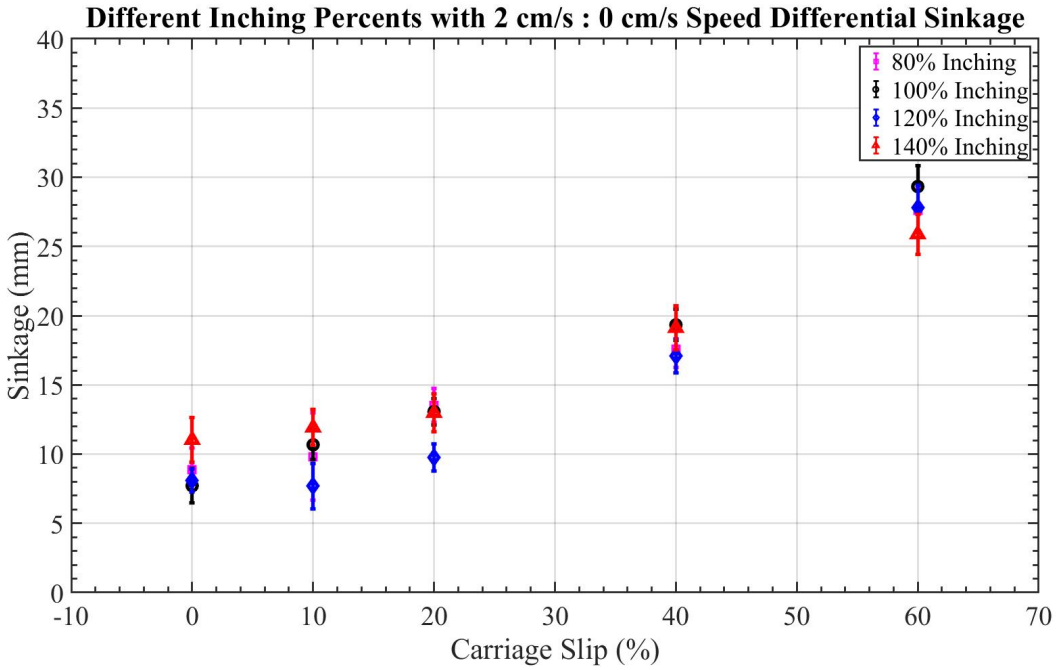

Figure 7.2: Sinkage values of different inching percentage tests

7.1 Summary

Sinkage is therefore shown to be fairly consistent at constant slip between inching and baseline tests. Sinkage differences in the past were shown when constant force held the system back, the baseline test sunk and stopped moving forward, achieving 100% slip. Whereas the inching could pull the system out of this stuck state. This shows the increased drawbar ability of the inching system but does not actually speak to a sinkage difference between the systems at the same slip.

Chapter 8

Conclusion

8.1 Summary of Work

Inching has been studied to a limited extent as a potential method of mobility for planetary rovers. However it was not well understood why it performed so much better than traditional methods of mobility and how that performance would change as various parameters were altered.

Over 100 tests were run in a sand testbed with a two-wheel mechanism to characterize inching mobility performance. These tests show that at low slips below 20% slip baseline tests outperform the inching tests. This is due to the varying speed nature of this inching mechanism causing at low slips the carriage to push the inching mechanism and induce negative slips at the end of each inching cycle. If this was all properly synchronized to achieve constant carriage slip these tests would actually perform similarly as was shown with self propelled tests.

At high slip values, anything above 20% slip, the inching dramatically outperforms the baseline tests. As the inching contracts it is similar in performance to baseline tests, however the expanding cycle performs considerably better and makes the average drawbar pull values of the inching much higher than the baseline tests.

Inching Percent was also investigated to understand how that parameter can affect performance. It was found that there is a peak drawbar achievable for each wheel slip. As this wheel slip increases so does the maximum drawbar pull achievable, similarly to single wheel and baseline test curves. However, this maximum drawbar is not achieved when the stationary wheel is not pushed backwards at 0.2 cm/s or faster. Pushing the stationary wheel backwards even faster does not produce higher results, anything about 0.2 cm/s performs exactly the same at any given wheel slip.

Driving the rear wheel faster without inching produced better drawbar pull coefficient results than baseline tests. If inching is not possible this is another way to get some performance benefits.

Sinkage data was compared as well and it was shown that at constant slip there was no difference between inching and baseline sinkage.

8.2 Contributions to Planetary Robotics

This thesis advances the understanding of planetary robotics mobility systems in the following ways:

- A working testbed was built that could collect data and test the inching, or push roll, drive type. This testbed includes a physical two-wheel mechanism that was mounted in an existing sand testbed. The testbed also includes new software to control this mechanism, and execute tests while logging all the data from the test. Finally an easy interface was built to gather data from any tests run and display it in an easily interpretable graph.
- Data was collected on over 120 tests using this testbed. These tests cover a wide range of varied parameters. All the motor speed data, six axis of force data, and sinkage data was stored in a database for future use and analysis.
- Finally, analysis is presented of all these test runs to characterize how individual parameters affect inching mobility system performance. Analysis is offered for how wheel speed affects performance, how carriage slip affects performance, how inching percent affects performance, and how adding this inching motion compares to baseline tests. Tests are also analyzed over time, reveling insights into why the inching performs the way it does and how inching performance varies over time.
- Tests are also run and analyzed where no inching occurs but wheels are driven at different speeds to start to understand how some benefits obtained by inching can be obtained without the need to inch.

8.3 Future Work

These results show promise that the inching method of mobility could increase planetary rover mobility systems. Due to these results the next steps include running even more tests with the two-wheel mechanism. It would also be important to modify and fine tune the controller running the testbed to understand how that affects the test results. A planner should also be built that could take advantage of this new method of mobility.

8.3.1 Tests To be Added

Tests were run to characterize how the baseline test would perform between 0% and 60% slip. However to further understand and confirm theories about baseline performance, tests could be run every 5% slip and tests could be run up to 90% slip. By adding these tests, the range of slips will be more fully characterized and understood. These tests are outlined in Figure 8.1.

Inching % = 0 for all tests			Wheel Speeds	
			1 (cm/s)	0.5 (cm/s)
Inching % = 0 for all tests	Carriage Slip %	5%	X	
		15%	X	
		25%	X	
		30%	X	X
		35%	X	
		45%	X	
		50%	X	
		55%	X	
		65%	X	
		70%	X	
		75%	X	
		80%	X	
		85%	X	
		90%	X	X

Figure 8.1: Future baseline tests to be run

Along with extended baseline tests, more perfect inching tests could also fill out the inching versus baseline graph more fully. These extended tests would confirm the performance follows assumed trends between all the slip values that were tested. More tests would also help to confirm exactly where the inching test performance starts to level off. These tests are outlined in Figure 8.2.

Inching % = 100 for all tests			Wheel Speed Slow:Fast(cm /s)		
			0 : 1	0 : 2	1 : 3
Perfect Inching Two Wheels at various speeds	Carriage Slip %	5%		X	X
		15%		X	X
		25%		X	X
		30%	X	X	X
		35%		X	X
		45%		X	X
		50%		X	X
		55%		X	X
		65%		X	X
		70%		X	X
		75%		X	X
		80%		X	X
		85%		X	X
		90%	X	X	X

Figure 8.2: Future perfect inching tests to be run

Finally, in the future it would be necessary to further fill out Figure 5.12. To fill out the graph with higher wheel slips, tests should be run at lower inching percent, and higher carriage percent. Since in these tests, when analyzed with respect to wheel slip instead of carriage slip, the highest wheel slip reached is only 40% it would be necessary to confirm trends by extending these tests into higher wheel slip values. This would prove test grouping even at higher slips and would show more clearly what slip value the leveling off of performance starts. These tests are outlined in Figure 8.3.

Wheel Speed Slow:Fast(cm /s) = 0 -> 2 for all tests			Inching %		
			60%	40%	90%
Varied Inching % and Cariage Slip %	Carriage Slip %	0%	X	X	X
		10%	X	X	X
		20%	X	X	X
		40%	X	X	X
		60%	X	X	X
		80%	X	X	X

Figure 8.3: Future varied inching percent tests to be run

While these tests aren't necessary to draw the conclusions in this work, they would be helpful to confirm further the conclusions and to make some of the trends more obvious by filling in holes.

8.3.2 Control

The controller used for the inching testbed was functional but simplistic. All motors were driven at the desired speed until a limit switch was reached and then the new motor speeds were set. This caused the inching system to not be smooth and to have moments of stillness at the end of each cycle. In the future, optimized control could likely improve the overall performance, especially at lower slip values. Near the end of each cycle, it would be beneficial to slowly decrease or increase the speeds to their new desired speed to get a smoother transition. In the future working to develop a smooth controller for the inching testbed would potentially produce better results and would also be more realistic to how an actual rover system would want to inch.

8.3.3 Planning with Inching

Now that inching has been more fully characterized it can begin to be experimented with as a possible future planetary rover drive system. In order to do this a planner would need to be built and tested that could utilize the various inching parameters to get the performance needed to drive over any given terrain. Given a necessary drawbar pull and natural sinkage, the inching percentage could be determined to achieve the desired drawbar pull.

Bibliography

[1] "Designing new ways to drive on mars," Jul 2004. (document), 1.1

[2] "Mars exploration rovers update: Spirit begins hibernation probably, opportunity roves on to endeavour crater," Mar 2010. (document), 1.2

[3] "'scarecrow' descends hill." (document), 1.3

[4] "Curiosity's tracks across dingo gap." (document), 1.4

[5] S. Moreland, K. Skonieczny, D. Wettergreen, V. Asnani, C. Creager, and H. Oravec, "Inching locomotion for planetary rover mobility," in *2011 Aerospace Conference*, pp. 1–6, IEEE, 2011. (document), 1.3, 1.6, 1.7

[6] C. Creager, K. Johnson, M. Plant, S. Moreland, and K. Skonieczny, "Push–pull locomotion for vehicle extrication," *Journal of Terramechanics*, vol. 57, pp. 71–80, 2015. (document), 1.3, 1.8

[7] D. A. Harrison, R. Ambrose, B. Bluethmann, and L. Junkin, "Next generation rover for lunar exploration," in *2008 IEEE aerospace conference*, pp. 1–14, IEEE, 2008. (document), 2.2, 2.1

[8] B. H. Wilcox, "Athlete: A cargo and habitat transporter for the moon," in *2009 IEEE Aerospace conference*, pp. 1–7, IEEE, 2009. (document), 2.2, 2.2

[9] P. Bartlett, D. Wettergreen, and W. Whittaker, "Design of the scarab rover for mobility & drilling in the lunar cold traps," 2008. (document), 2.2, 2.3

[10] W. CARRIER, III, "Soviet rover systems," in *Space Programs and Technologies Conference*, p. 1487, 1992. 1.1

[11] J. P. Grotzinger, J. Crisp, A. R. Vasavada, R. C. Anderson, C. J. Baker, R. Barry, D. F. Blake, P. Conrad, K. S. Edgett, B. Ferdowski, *et al.*, "Mars science laboratory mission and science investigation," *Space science reviews*, vol. 170, no. 1-4, pp. 5–56, 2012. 1.1, 4.1

[12] M. Maimone, J. Biesiadecki, E. Tunstel, Y. Cheng, and C. Leger, "Surface navigation and mobility intelligence on the mars exploration rovers," *Intelligence for Space Robotics*, pp. 45–69, 2006. 1.1, 2.1, 4.1

[13] M. Heverly, J. Matthews, J. Lin, D. Fuller, M. Maimone, J. Biesiadecki, and J. Leichty, "Traverse performance characterization for the mars science laboratory rover," *Journal of Field Robotics*, vol. 30, no. 6, pp. 835–846, 2013. 1.1, 1.1, 4.1

[14] R. A. Lindemann and C. J. Voorhees, "Mars exploration rover mobility assembly design, test and performance," in *2005 IEEE International Conference on Systems, Man and Cybernetics*, vol. 1, pp. 450–455, IEEE, 2005. 1.1

[15] R. A. Kerr, "Mars rover trapped in sand, but what can end a mission?," 2009. 1.1

[16] D. Brown and G. Webster, "Now a stationary research platform, nasas mars rover spirit starts a new chapter in red planet scientific studies," *Retrieved June*, vol. 16, p. 2010, 2010. 1.1

[17] S. J. Moreland, *Traction Processes of Wheels on Loose, Granular Soil*. PhD thesis, Doctoral Dissertation, Carnegie Mellon University, 2013. 1.3, 2.3, 2.5, 2.5, 3.1, 5.1

[18] M. Golombek, R. Anderson, J. R. Barnes, J. Bell, N. Bridges, D. Britt, J. Brückner, R. Cook, D. Crisp, J. Crisp, *et al.*, "Overview of the mars pathfinder mission: Launch through landing, surface operations, data sets, and science results," *Journal of Geophysical Research: Planets*, vol. 104, no. E4, pp. 8523–8553, 1999. 2.1

[19] R. E. Arvidson, S. W. Squyres, R. C. Anderson, J. F. Bell, D. Blaney, J. Brueckner, N. A. Cabrol, W. M. Calvin, M. H. Carr, P. R. Christensen, *et al.*, "Overview of the spirit mars exploration rover mission to gusev crater: Landing site to backstay rock in the columbia hills," *Journal of Geophysical Research: Planets*, vol. 111, no. E2, 2006. 2.1

[20] S. W. Squyres, R. E. Arvidson, D. Bollen, J. F. Bell III, J. Brueckner, N. A. Cabrol, W. M. Calvin, M. H. Carr, P. R. Christensen, B. C. Clark, *et al.*, "Overview of the opportunity mars exploration rover mission to meridiani planum: Eagle crater to purgatory ripple," *Journal of Geophysical Research: Planets*, vol. 111, no. E12, 2006. 2.1

[21] A. Vasavada, J. Grotzinger, R. Arvidson, F. Calef, J. Crisp, S. Gupta, J. Hurowitz, N. Mangold, S. Maurice, M. Schmidt, *et al.*, "Overview of the mars science laboratory mission: Bradbury landing to yellowknife bay and beyond," *Journal of Geophysical Research: Planets*, vol. 119, no. 6, pp. 1134–1161, 2014. 2.1

[22] K. Skonieczny, S. J. Moreland, and D. S. Wettergreen, "A grouser spacing equation for determining appropriate geometry of planetary rover wheels," in *2012 IEEE/RSJ International Conference on Intelligent Robots and Systems*, pp. 5065–5070, IEEE, 2012. 2.1, 2.5, 3.1

[23] N. Patel, R. Slade, and J. Clemmet, "The exomars rover locomotion subsystem," *Journal of Terramechanics*, vol. 47, no. 4, pp. 227–242, 2010. 2.2

[24] L. Ding, Z. Deng, H. Gao, K. Nagatani, and K. Yoshida, "Planetary rovers' wheel—soil interaction mechanics: new challenges and applications for wheeled mobile robots," *Intelligent Service Robotics*, vol. 4, no. 1, pp. 17–38, 2011. 2.3

[25] K. Yoshida, T. Watanabe, N. Mizuno, and G. Ishigami, "Terramechanics-based analysis and traction control of a lunar/planetary rover," in *Field and Service Robotics*, pp. 225–234, Springer, 2003. 2.3, 2.4

[26] K. Yoshida and H. Hamano, "Motion dynamics of a rover with slip-based traction model," in *Proceedings 2002 IEEE International Conference on Robotics and Automation (Cat. No. 02CH37292)*, vol. 3, pp. 3155–3160, IEEE, 2002. 2.3

[27] M. Bekker, "Introduction to terrain-vehicle systems. 1969," *Ann Arbor, MI: University of*

Michigan Press. 2.3

[28] D. R. Freitag, A. J. Green, and K.-J. Melzer, "Performance evaluation of wheels for lunar vehicles," tech. rep., ARMY ENGINEER WATERWAYS EXPERIMENT STATION VICKSBURG MS, 1970. 2.3

[29] D. R. Freitag, "A dimensional analysis of the performance of pneumatic tires on soft soils.," tech. rep., ARMY ENGINEER WATERWAYS EXPERIMENT STATION VICKSBURG MS, 1965. 2.3

[30] R. Bauer, W. Leung, and T. Barfoot, "Experimental and simulation results of wheel-soil interaction for planetary rovers," in *2005 IEEE/RSJ international conference on intelligent robots and systems*, pp. 586–591, IEEE, 2005. 2.4

[31] M. Ono, T. J. Fuchs, A. Steffy, M. Maimone, and J. Yen, "Risk-aware planetary rover operation: Autonomous terrain classification and path planning," in *2015 IEEE Aerospace Conference*, pp. 1–10, IEEE, 2015. 4.1